

Cost-optimal Management of a Residential Heating System With a Geothermal Energy Storage Under Uncertainty

Paul Honore Takam ¹ Ralf Wunderlich ¹

¹ Brandenburg University of Technology Cottbus-Senftenberg, Institute of Mathematics, P.O. Box 101344, 03013 Cottbus, Germany;

* **Correspondence:** ralf.wunderlich@b-tu.de

Abstract: In this paper, we consider a residential heating system with renewable and non-renewable heat generation and different consumption units and investigate a stochastic optimal control problem for its cost-optimal management. As a special feature, the heating system is equipped with a geothermal storage that enables the intertemporal transfer of thermal energy by storing surplus heat for later use. In addition to the numerous technical challenges, economic issues such as cost-optimal control also play a central role in the design and operation of such systems. The latter leads to challenging mathematical optimization problems, as the response of the storage to charging and discharging decisions depends on the spatial temperature distribution in the storage. We take into account uncertainties regarding randomly fluctuating heat generation from renewable energies and the environmental conditions that determine heat demand and supply. The dynamics of the multidimensional controlled state processes is governed by a partial, a random ordinary and two stochastic differential equations. We first apply a spatial discretization to the partial differential equation and use model reduction techniques to reduce the dimension of the associated system of ordinary differential equations. Finally, a time-discretization leads to a Markov decision process for which we apply a state discretization to determine approximations of the cost-optimal control and the associated value function.

Keywords: Stochastic optimal control, Markov decision process, Geothermal energy storage, Model order reduction, Residential heating system, Numerical simulation

Mathematics Subject Classification: 93E20 90-08 90C40 91G60

1. Introduction

Climate change and energy dependency require urgent measures for the improvement of energy efficiency in all areas. District heating and cooling systems play an important role for increasing energy efficiency in buildings and for including renewable energy sources. In addition to numerous technical issues, economic questions such as the cost-optimal control and management of such heating systems

also play a central role. The latter leads to challenging mathematical optimization problems which require advanced and sophisticated solution techniques. One of these problems arising in the optimal management of a residential heating system with access to an additional geothermal energy storage (GES), as depicted in Fig. 1.1, is addressed in this paper.

Thermal storage facilities and in particular geothermal energy storage help to mitigate and to manage temporal fluctuations of heat supply and demand for heating and cooling systems of single buildings as well as for district heating systems. They make it possible to store heat in the form of thermal energy and to use it again hours, days, weeks or months later. This is attractive for space heating, domestic or process hot water production, or generating electricity, since it improves the efficiency and saves costs. Geothermal storage are becoming increasingly important and are very attractive for heating systems in residential buildings, as they are very economical to build and maintain. Furthermore, such storage can be integrated both in new buildings and in renovations. GES can also be used to cushion peaks in the electricity grid by converting electrical energy into thermal energy (power to heat). Pooling several GESs within the framework of a virtual power plant gives the necessary capacity which allows to participate in the balancing energy market.

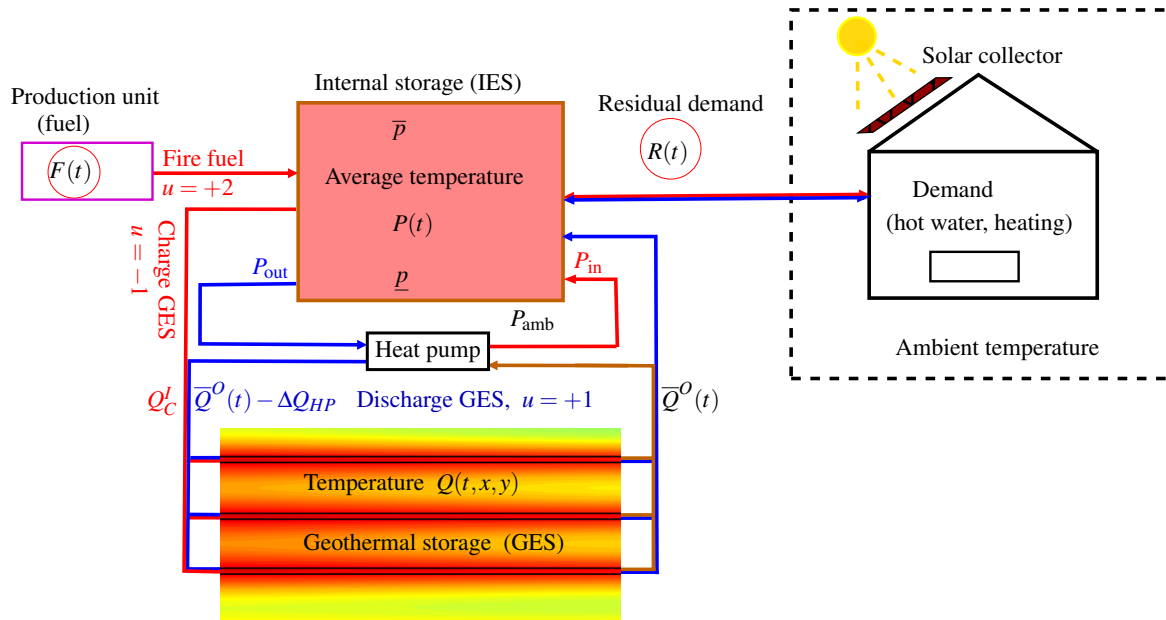


Figure 1.1. Simplified model of a residential heating system. Sect. 2 introduces the notation and gives explanation.

In the GES investigated in this work, a certain volume under or adjacent to a building is filled with soil and insulated from the surrounding ground. The thermal energy is stored by increasing the temperature of the soil inside the storage tank. It is charged and discharged through pipe heat exchangers (PHX) filled with a liquid such as water. The fluid carrying the thermal energy is moved using pumps. The PHXs are connected to an internal energy storage (IES) which is—as a water tank. Contrary to the GES, the IES has a smaller capacity and is designed to buffer imbalances of heat supply and demand in the heating system on short time scales. In addition, the GES stores heat at a lower temperature level, so heat pumps must be used for heat transfer from the GES to the IES.

A special feature of the GES considered in this paper is that, it is not insulated at the bottom,

allowing thermal energy to flow into deeper layers. This is a natural extension of the storage capacity, as this heat can be recovered to some extent if the GES is sufficiently discharged (cooled) and a heat flow is induced back into the storage. Of course, there are inevitable diffusion losses to the environment, but due to the open architecture, the GES can take advantage of higher temperatures in deeper layers of the ground and acts as a production unit similar to a downhole heat exchanger.

In this work, we consider a mathematical model of a residential heating system consisting of

- a local renewable heat production unit such as a solar thermal collector,
- a non-renewable heat production unit such as a fuel-fired boiler,
- several heat consumption units in the building,
- an internal energy storage, that serves as a short-term buffer storage and is typically realized as a water tank,
- and, as a special feature, a geothermal storage with large capacity, which can store energy for longer periods.

In this model, we do not describe all the technical details of heat transfer to and from the consumption units of the building and the contribution of the solar collector. Instead, we only consider the aggregated residual demand describing the imbalance of the intermittent demand for thermal energy in the building and the supply of thermal energy from local production of solar collector. This residual demand generally does not only fluctuate over time, but its future values cannot be predicted with certainty, as they depend on the weather-dependent heat production of the solar collector and the demand behavior of consumers. Therefore, we model it using a stochastic process. Further, depending on the size of the heating system and the selected tariff for the fuel purchase, this also applies to the future fuel price, which may depend on the situation on the energy market. Therefore, like residual demand, we also model the fuel price as a stochastic process.

From an economic point of view, the aim is to operate the heating system in such a way that the aggregated costs of purchasing fuel and the electricity costs for operating the system, in particular for the transfer of heat between the IES and GES using heat pumps, are minimized over a certain period of time. These minimum costs must be known in order to make decisions about investing in certain heating systems or the size of an additional external geothermal storage. The optimal operation of the heating system, including the interaction of the two storage systems IES and GES, is a decision-making problem under uncertainty, since the control decisions must be made in the face of uncertainty about future energy prices and future residual demand. We will formulate it mathematically as a stochastic optimal control problem.

In contrast to the typical situation in continuous-time stochastic control theory, where the dynamics of the controlled state is determined by a system of stochastic and ordinary differential equations (SDEs and ODEs), one of the state components is described by a heat equation with convection, that is a parabolic partial differential equation (PDE). This is a non-standard feature of the control problem that requires special attention. The reason for the inclusion of the heat equation is that the GES response to charging and discharging operations depends on the spatial temperature distribution in the storage medium, in particular in the vicinity of the PHX. The dynamics of this distribution is described by the heat equation. Please note that when charging the GES, the liquid in the PHX reaches the GES inlet at a high temperature from the IES. On its way through the GES, the heat of the fluid is transferred to the colder storage medium and it returns to the IES at a lower temperature. A heat pump is used

for transferring heat from the GES to the IES. It consists of two circuits. In the first circuit, heat is extracted from the GES by sending the fluid through the PHX at a low temperature so that it can absorb heat from the surrounding medium and return to the heat pump at a higher temperature. There, heat is extracted from the fluid in the first circuit and transferred to the fluid in the second circuit. In addition, the temperature is increased by using additional electrical energy so that it can be sent to the IES at a level suitable for the heating system.

Due to this mode of operation of the charging and discharging processes, heat transfer from the IES to the GES is delayed when the PHX environment is saturated and at a high temperature. In this case, the fluid in the PHX exits the GES at an almost identical temperature to its initial entry, with only a negligible amount of heat transferred to the storage medium. In order to save costs for operating the pumps, it is advantageous in such a case to stop the charging process first and instead wait until the heat in the immediate vicinity of the PHX has spread to colder regions within the GES. Vice versa, the heat transfer from the GES to the IES becomes inefficient if there is a non-homogeneous temperature distribution with low temperatures in the PHX environment. Then, the fluid in the PHX can only absorb a small amount of heat from the storage medium.

Literature review on geothermal energy storage. We refer to Dincer and Rosen [8] and Regnier et al. [24] for an overview on thermal energy storage. The work of Guelpa and Verda [13] and Kitapbayev et al. [15] showed that thermal energy storage can significantly increase both the flexibility and the performance of district energy systems and enhancing the integration of intermittent renewable energies into thermal networks. The article Major et al. [17] considered heat storage capabilities of deep sedimentary reservoirs. Here, the governing heat and flow equations are solved using finite element methods. Further contributions on the numerical simulation of such storage are provided in [5, 26].

The GES examined in this article is a relatively new and specialized technology that has been developed and used only in the last 15 years. To our knowledge, there are only a few references such as [1, 2, 31, 29, 30, 28] which deal with the mathematical modeling and numerical simulation of such storage facilities. However, the heat transfer and exchange processes between the heat exchanger and the surrounding soil also play a crucial role not only in this work, but also for so-called ground source heat pumps. They extract heat from the ground and feed it into heating systems. However, a storage function is of little or no importance here. There is a large amount of specialist literature on modeling and simulation for these systems, which are divided into horizontal and vertical geothermal heat exchangers. An overview can be found in Zayed et al. [34].

Literature review on optimal energy storage management. Energy storage can be used to create profit by trading in the energy market and taking advantage of the fluctuating energy price by applying an active storage management, see B auerle and Riess [4], Chen and Forsyth [6, 7], Ware [33], Shardin and Wunderlich [25]. The basic principle is to buy and store energy when prices are low, and to release and sell energy when market prices are high, and to keep the intermediate storage and operating costs, and unavoidable dissipative losses under control.

Literature review on optimal management of heating systems. The residential heating system studied in this work can be considered as a thermal microgrid. This is an autonomous energy system with local thermal energy generation and storage units used to meet the heating demand. There is an extensive literature on the topic of optimal management of electrical microgrids. Some of these articles also include thermal units in the microgrid and investigate combined heat and electricity systems. In Testi et al. [32], an optimal integration of electrically driven heat pumps within a hybrid distributed energy

system is investigated. There, the authors proposed a multi-objective stochastic optimization methodology to evaluate the integrated optimal sizing and operation of the energy systems under uncertainties in climate, space occupancy, energy loads, and fuel costs. In Kuang et al. [16], a stochastic dynamic solution for off-design operation optimization of combined heating and power systems with energy storage is considered. In Gu et al. [12], a review on optimal energy management of combined cooling, heating and power microgrid is considered. Further contributions on combined heating, cooling, and power system are given in [9, 35] and references therein.

Literature review on stochastic optimal control. As already mentioned, the cost-optimal management of a heating system for residential buildings under uncertainty is treated mathematically as a stochastic optimal control problem. A large body of literature on this theory investigates *dynamic programming* solution techniques. In the continuous-time setting, where diffusion or jump-diffusion processes form the controlled state process, this leads to the Hamilton-Jacobi-Bellman equation as a necessary optimality condition, see Fleming and Soner [10], Pham [20], and Oksendal and Sulem [18]. These nonlinear PDEs can usually only be solved with *numerical methods*, as in Shardin and Wunderlich [25], Chen and Forsyth [7].

For discrete-time models, the theory of Markov decision processes (MDPs) offers a solutions based on backward recursion. We refer to Bäuerle and Rieder [3], and Puterman [23], Hernández-Lerma and Lasserre [14] and Powell [22]. Such MDPs also result from time discretisation of continuous-time control problems.

Our contribution. This article presents a comprehensive mathematical approach for modelling the operation of a heating system equipped with a GES in residential buildings, which makes it possible to formulate and solve optimization problems that arise in the cost-optimal management of such systems. It explicitly takes into account the stochasticity of the imbalance of heat supply and demand due to intermittent heat production of the solar collector and the fluctuating demand behavior of consumers, as well as fluctuating market prices for fuel. These variables are modeled by suitable stochastic processes. Further, the model captures the dynamics of the spatial temperature distribution in the GES which is described by a heat equation with convection term. This enables a precise description of the interaction between the two storage units, IES and GES, and the response of the GES to charging and discharging processes, which is necessary to control the heating system.

The cost-optimal management of the heating system based on the continuous-time setting leads to a non-standard stochastic optimal control problem in which the dynamics of the continuous-time state process is described by a system of two SDEs, one ODE and one PDE. Therefore, we first approximate the dynamics of the spatial GES temperature distribution determined by the PDE by a low-dimensional system of ODEs combining semi-discretization of the PDE and model order reduction techniques. In a second step, we perform a time discretization that leads to state dynamics described by a system of random recursions. While the controls between two discrete points are assumed to be constant, the dynamics of the state variables in each of the periods are still analyzed in continuous time to avoid unnecessary time discretization errors.

This approach enables the cost-optimal management problem to be treated as an MDP. Since the solution of MDP with dynamic programming methods is confronted with the curse of dimensionality due to the high dimension of the state space, we approximate the MDP by another MDP for a discretized state space. This finally enables an efficient computation of the approximation of the value function and the optimal decision rules for which we provide numerical results.

Paper organization. Sect. 2 provides a description of the residential heating system. In Sect. 3, the state and control variables are introduced. Sect. 4 is devoted to the continuous-time dynamics of the controlled state process which is governed by a system of ODEs, SDEs and a PDE. In Sect. 5, we consider the approximation of the dynamics of the spatial temperature distribution in the GES by a low-dimensional system of ODEs. In Sect. 6, we formulate the stochastic optimal control problem as an MDP. An approximate method to solve the MDP which is based on a state discretization is studied in Sect. 7. In Sect. 8, we present numerical results which show properties of the value function and the optimal decision rules. The paper concludes in Sect. 9 with a short summary and outlook. An appendix provides a list of notations and collects proofs and technical results that have been removed from the main text.

2. Residential Heating System

A residential heating system is designed to provide thermal energy for heating and hot water supply of a building. Here, the notion “building” is used for single family homes, office buildings, small companies or even small districts with a couple of buildings sharing a common heat and water supply.

Residual demand. The building is equipped with some local production units for thermal energy such as solar collectors or other units using renewable energies. The supply of these units usually does not meet exactly the demand of thermal energy due to the immanent temporal fluctuations and seasonality effects in both supply and demand. We call that imbalance the residual demand, and model it by a stochastic process $\tilde{R} = (\tilde{R}(t))_{t \in [0, T]}$, which we decompose as $\tilde{R}(t) = \mu_R(t) + R(t)$. Here, μ_R denotes the deterministic seasonality, a regular, repeating pattern known from historical data, while the stochastic process R is the deseasonalized component describing the uncertain future deviations from the seasonality pattern. More details will be given below in Subsect. 4.1.

Internal energy storage. If the demand exceeds the supply from local production then the excess demand $\tilde{R}(t) > 0$ is satisfied by an internal buffer storage. It also stores overproduction of thermal energy which is not needed to satisfy the demand. In that case $\tilde{R}(t)$ is negative. This internal storage is designed to balance supply and demand on shorter time scales of some hours or only few days. However, the capacity is not sufficient to serve as buffer for seasonal fluctuations on time scales of weeks and months.

As often observed in reality, we assume the internal buffer storage to be a stratified hot water storage tank. The warmest storage layer is at the top and below there are colder layers through natural layering. For simplicity, we assume that the storage can keep a constant temperature \bar{p} on the top and also a constant temperature $\underline{p} < \bar{p}$ at the bottom. We do not model the vertical temperature profile in the storage but consider only the storage’s average temperature which is denoted by $P(t)$ for time $t \in [0, T]$.

Fuel-fired boiler. Due to its limited capacity, the internal storage cannot provide the necessary heat supply for a permanent or very strong unsatisfied demand of the building. Therefore, the system is equipped with another production unit, which is able to generate enough heat also on short time scales and to prevent the internal storage to become completely empty. This unit may fire fossil fuels (gas, oil, coal), convert electricity to heat using an immersion heater or obtain additional heat from a district heating system as in [11]. In all cases, this heat production comes with additional costs arising from the consumption of fuel, or electricity, or other respective heat sources. To be more specific, we

call this additional production unit a “fuel-fired boiler” and the price of the respective heat source a “fuel price”, keeping alternative energy sources in mind. We denote this fuel price at time t by $\tilde{F}(t)$. Uncertainties about the future prices will be captured by modeling \tilde{F} as a stochastic process, which we decompose, as in the case of the residual demand, into $\tilde{F} = \mu_F + F$ with the deterministic seasonality pattern μ_F and deseasonalized stochastic component F . For more details we refer to Subsect. 4.1.

Geothermal energy storage. In periods of permanent or strong overproduction, the internal storage may reach its capacity limits and can no longer accommodate more leftover heat from the local production. In order to enable a later usage of that leftover heat, the heating system is equipped with an additional external thermal storage, which in this work is a geothermal storage. Compared to the internal storage, its capacity is much larger, but it is also characterized by a lower temperature level. Therefore, heat pumps are required for transferring heat from the geothermal to the internal storage. Further, the transfer of thermal energy to and from the external storage depends on the often slow operation of heat exchangers. The geothermal storage is characterized by a nonhomogeneous spatial and temporal temperature distribution. We will work with a spatially two-dimensional model and denote by $Q(t, x, y)$ the GES temperature at time t and the point (x, y) . More details are provided in Subsec. 4.2.

If the internal storage is already (almost) fully charged and there is still overproduction of thermal energy in the building, then heat can be transferred from the internal to the external storage. This is achieved by sending a fluid of high temperature from the internal storage tank through the heat exchanger pipes of the geothermal storage tank. The fluid arrives at the (possibly multiple) inlets of the pipe heat exchangers (PHXs) with the inlet temperature denoted by $Q^I(t)$. After passing through the geothermal storage, the fluid will leave the PHXs with a lower temperature. The average temperature at the (possibly multiple) outlets is denoted by $\bar{Q}^O(t)$, see below Eq. (4.10) for details. This is also the temperature at which the fluid returns to the internal storage. Since the efficiency of charging the geothermal storage is improved by increasing the inlet temperature $Q^I(t)$, we assume in this work that during charging, this temperature is equal to the maximum available temperature provided by the system, which we denote by the constant Q_C^I .

On the other hand, if the internal storage is (almost) empty and there is still unsatisfied demand in the building, then instead of producing heat from firing fuel, thermal energy can also be transferred from the geothermal storage to the internal storage. For that process, the system uses a *heat pump* for raising the temperature of the fluid arriving from the outlet of the geothermal storage to a higher level $P_{\text{in}} > \underline{p}$. Here P_{in} is a pre-specified temperature at which the fluid coming from the heat pump arrives at the internal storage. For simplicity, we assume that P_{in} is constant.

The heat pump connects two circuits in which moving fluids carry heat. A first circuit is connected to the geothermal storage. The fluid arrives from the storage’s outlet at the inlet of the heat pump with temperature \bar{Q}^O . The heat pump withdraws heat from the fluid so that it leaves the pump at time t with the temperature $\bar{Q}^O(t) - \Delta T_{HP}$, and returns to the inlet of the geothermal storage. The quantity $\Delta T_{HP} > 0$ is called heat pump spread and assumed to be a given constant. The thermal energy extracted from the fluid of the first circuit is transferred to the fluid in the second circuit. The latter connects the heat pump with the internal storage. At the pump’s inlet arrives cold water of temperature P_{out} , which is raised to the temperature $P_{\text{in}} > P_{\text{out}}$, that is suitable for the heating system, using the extracted heat in the first circuit and additional electrical energy. At this temperature, the fluid returns to the internal storage.

3. Control System

In this section we setup the model for continuous-time $t \in [0, T]$, where $T > 0$ is a finite time horizon.

State. The state of the control system at $t \in [0, T]$ is given by the following four quantities. First, P the average temperature in the IES and Q , the spatio-temporal temperature distribution in the geothermal storage are the controlled or endogeneous state components. Further, the deseasonalized residual demand R and the deseasonalized fuel price F are two uncontrolled or exogeneous state components which will be modeled as stochastic processes. We define the state process by $X = (R, F, P, Q)'$ where x' denotes the transpose of the vector x . Further details and the description of the state dynamics are given below in Sect. 4.

Control. The operator or decision maker for the considered residential heating system has several control actions at his disposal which relate to the charging and discharging operations of the two storage facilities. The GES is charged and discharged via the PHXs connected to the IES and filled with some fluid. We assume that during such charging and discharging operations the fluid in the PHX is always moving with the constant velocity $\bar{v}_0 > 0$. The GES is charged by transferring heat from the IES, and vice versa it is discharged by transferring heat to the IES. The IES can also be charged by firing fuel. We assume that simultaneous discharging or charging the GES and firing fuel is not allowed, since it will not generate minimum cost and will be therefore not optimal. If both the IES and GES are full, and there is an overproduction of heat by the solar collector, that is the residual demand is negative, then the operator no longer can store this energy but has to discard it. We will call this control action *over-spilling* and assume that it is associated with zero costs and that during over-spilling the temperature of the IES will remain constant at the maximum temperature \bar{p} .

We formalize this by introducing the *set of feasible actions*

$$\mathcal{K} = \{-2, -1, 0, +1, +2\} \quad (3.1)$$

from which the decision maker can select at any time $t \in [0, T]$ an control action and form the *continuous-time control process* $u : [0, T] \rightarrow \mathcal{K}$. The interpretation of the actions in \mathcal{K} is as follows. The action $+1$ indicates charging the IES by transferring heat from the GES, whereas -1 denotes discharging the IES by transferring heat to the GES. In both cases the fuel-fired boiler is off. The action $+2$ indicates that heat is generated by firing fuel to charge the IES, with the PHX pumps switched off. The action 0 means wait or suspend, whereby both the PHX pumps and the fuel-fired boiler are switched off. Finally, -2 denotes over-spilling.

4. State Dynamics

In this section, we describe the dynamics of each individual component of the state process X . We start with the residual demand R and the fuel price F which we model as stochastic processes satisfying SDEs. Then we derive a PDE for the spatio-temporal temperature distribution in the geothermal storage given by Q . Finally, we consider the average temperature in the internal storage P which is governed by an ODE.

4.1. Residual Demand and Fuel Price

The two exogenous states describing the deseasonalized residual demand R and the deseasonalized fuel price F are modeled as stochastic processes defined on a filtered probability space $(\Omega, \mathcal{G}, \mathbb{G}, \mathbb{P})$. In particular, that space supports a two-dimensional standard Wiener process $W = (W_R, W_F)'$ on $[0, T]$ driving the SDEs (4.2) for R and (4.4) for F given below. The filtration \mathbb{G} is assumed to be generated by W , that is, $\mathbb{G} = \mathbb{G}^W = (\mathcal{G}^W(t))_{t \in [0, T]}$ with the σ -algebras $\mathcal{G}^W(t) = \sigma\{W(s), s \leq t\}$, augmented by the \mathbb{P} -null sets, so that, \mathbb{G} satisfies the usual assumptions of right-continuity and completeness.

Residual demand. Recall, the residual demand $\tilde{R}(t)$ describes the imbalance, i.e., the difference between the demand for thermal energy in the building and supply of thermal energy provided by the local production units at time $t \in [0, T]$, and is measured in kW . It can take positive as well as negative values in \mathbb{R} . The residual demand is positive if demand exceeds supply, and negative if supply exceeds demand (overproduction). For the formulation of the stochastic optimal control problem it will be useful to decompose the residual demand on $[0, T]$ as follows

$$\tilde{R}(t) = \mu_R(t) + R(t). \quad (4.1)$$

Here, $\tilde{\mu}_R : [0, T] \rightarrow \mathbb{R}$ is a bounded deterministic function describing the residual demand's seasonality, and $R = \tilde{R} - \mu_R$ is the deseasonalized residual demand, which we model as an Ornstein-Uhlenbeck process which is mean-reverting to zero, and defined by the SDE

$$dR(t) = -\beta_R R(t)dt + \sigma_R(t)dW_R(t), \quad R(0) = r_0 \in \mathbb{R}, \quad (4.2)$$

where W_R is a standard Wiener process. The parameter $\beta_R > 0$ is called mean-reversion speed and $\sigma_R : [0, T] \rightarrow [\underline{\sigma}_R, \overline{\sigma}_R]$ is a deterministic and bounded volatility function with some constants $0 < \underline{\sigma}_R \leq \overline{\sigma}_R$. The use of a time-dependent volatility function σ_R makes it possible to link the stochastic variability of \tilde{R} to certain seasonal patterns. Simple but already meaningful examples of the above-mentioned seasonality function have the form

$$\mu_R(t) = \mu_R^0 + \sum_{i=1}^M \mu_R^i \cos \frac{2\pi(t - t_R^i)}{\delta_R^i}, \quad (4.3)$$

where the constant $\mu_R^0 \in \mathbb{R}$ denotes the long-term mean, and $\mu_R^i > 0$, $i = 1, \dots, M$, the amplitude of the seasonality component, δ_R^i the length of the seasonal period and t_R^i some time shift parameter for the i -th seasonality component (representing the time of the seasonal peak of the residual demand) and M is the number of components.

Fuel price. Similarly to (4.1), the fuel price \tilde{F} is a stochastic process which can be decomposed as $\tilde{F}(t) = \mu_F(t) + F(t)$ where, μ_F is a bounded deterministic seasonality function. Typical examples are functions as in (4.3) but with only a yearly component and no daily component. The deseasonalized fuel price F is modeled by an Ornstein-Uhlenbeck process which is mean reverting to zero. It captures the random effects in the fuel price, and is defined by the SDE

$$dF(t) = -\beta_F F(t)dt + \sigma_F(t)dW_F(t), \quad F(0) = f_0 \in \mathbb{R}. \quad (4.4)$$

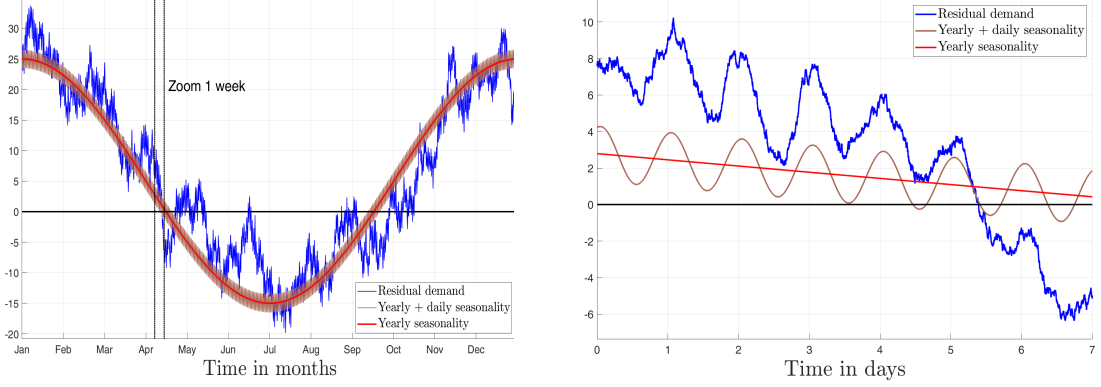


Figure 4.1. Residual demand \tilde{R} over a period of one year (left) and a zoom on a week in mid-April (right) with parameters $\beta = 0.5$, $\sigma^R = 2$, $\mu_R^0 = 5$, $\mu_R^2 = 20$, $\mu_R^1 = 1.5$, $\delta_R^1 = 365$ days, and $\delta_R^2 = 1$ day. Blue solid line for residual demand \tilde{R} , red and brown solid lines show the yearly component and the seasonality function μ_R with combined yearly and daily components. The long-term mean level μ_R^0 is shown as a black solid line.

Here, $\beta_F > 0$ denotes the mean-reversion speed, and $\sigma_F : [0, T] \rightarrow [\underline{\sigma}_F, \overline{\sigma}_F]$ is a deterministic and bounded volatility function with some constants $0 < \underline{\sigma}_F \leq \overline{\sigma}_F$. For further simplification, we can assume that the fuel price is a known deterministic function of time or even constant. Then the fuel price can be removed from the state variables of the control problem which reduces the dimension of the state space by one.

4.2. Spatio-temporal Temperature Distribution in the Geothermal Storage

The dynamics of the spatial temperature distribution in a geothermal storage can be described mathematically by a linear heat equation with convection term and appropriate boundary and interface conditions.

4.2.1. Two-dimensional Model

The setting is based on [31, Sect. 2]. For self-containedness and the convenience of the reader, we recall in this subsection the description of the model. The GES area is assumed to be a cuboid for which we consider a two-dimensional rectangular cross-section. As mentioned above $Q = Q(t, x, y)$ is the temperature at time $t \in [0, T]$ in the point $(x, y) \in \mathcal{D} = (0, l_x) \times (0, l_y)$ where l_x, l_y are the width and height of the storage. Fig. 4.2 depicts the domain \mathcal{D} and its boundary $\partial\mathcal{D}$. The domain \mathcal{D} is divided into three parts. The first \mathcal{D}^M is filled with the storage medium (soil) which is assumed to be homogeneous for simplicity, and characterized by the constant material parameters ρ^M , κ^M , and c_p^M denoting mass density, thermal conductivity and specific heat capacity, respectively. The second is \mathcal{D}^F , it represents the PHXs and is filled with a fluid (water) with constant material parameters ρ^F , κ^F and c_p^F . The fluid moves with time-dependent velocity $v_0(t)$ along the PHXs. For the sake of simplicity, we will restrict ourselves to the case frequently encountered in practice, where the pumps that move the liquid are either switched on or off. Thus, the velocity $v_0(t)$ is piecewise constant taking only the two values $\bar{v}_0 > 0$ and zero. Finally, the third part is the interface \mathcal{D}^J between \mathcal{D}^M and \mathcal{D}^F . We

neglect modeling the wall of the PHX and assume perfect contact between the PHX and the ground for simplicity. Details are given below in (4.8) and (4.9). We summarize as follows

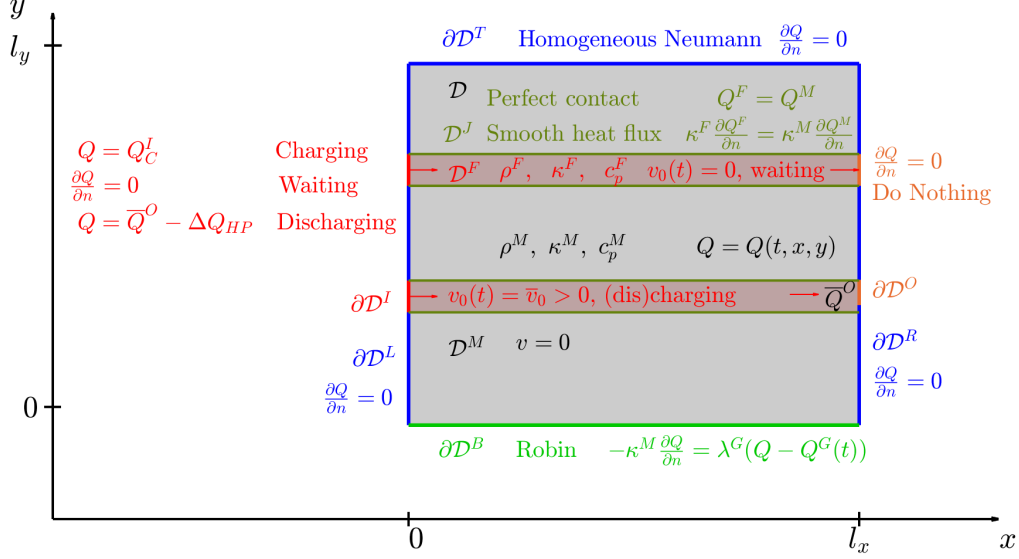


Figure 4.2. Two-dimensional model of the geothermal storage: decomposition of the domain \mathcal{D} , boundary and interface conditions. Red arrows indicate the direction of the flow.

Assumption 4.1.

1. Material parameters of the medium ρ^M, κ^M, c_p^M in the domain \mathcal{D}^M and of the fluid ρ^F, κ^F, c_p^F in the domain \mathcal{D}^F are constants.
2. Fluid velocity is piecewise constant, that is, $v_0(t) = \begin{cases} \bar{v}_0 > 0, & \text{pump on,} \\ 0, & \text{pump off.} \end{cases}$
3. Perfect contact and impermeability at the interface between fluid and medium.
4. $Q^G(t) \leq Q_C^I$ for all $t \in [0, T]$.

The last assumption ensures that the GES temperature and thus also the outlet temperature \bar{Q}^O is always bounded by the inlet temperature during charging Q_C^I . Note that the findings derived from our two-dimensional model, where \mathcal{D} is a rectangular cross-section of a box-shaped storage, can be also used for three-dimensional model under the assumption that the storage domain is a cuboid of depth l_z with a homogeneous temperature distribution in the z -direction.

Heat equation. The temperature $Q = Q(t, x, y)$ in the external storage is governed by the linear heat equation with convection term

$$\rho c_p \frac{\partial Q}{\partial t} = \nabla \cdot (\kappa \nabla Q) - \rho v \cdot \nabla (c_p Q), \quad (t, x, y) \in (0, T] \times \mathcal{D} \setminus \mathcal{D}^J,$$

where $\nabla = (\frac{\partial}{\partial x}, \frac{\partial}{\partial y})$ denotes the gradient operator. The first term on the right hand side describes diffusion, while the second represents convection of the moving fluid in the PHXs. Further, $v = v(t, x, y)$

$= v_0(t)(v^x(x,y), v^y(x,y))'$ denotes the velocity vector with $(v^x, v^y)'$ being the normalized directional vector of the flow. According to Assumption 4.1, the material parameters ρ, κ, c_p depend on the position (x,y) and take the values ρ^M, κ^M, c_p^M for points in \mathcal{D}^M (medium) and ρ^F, κ^F, c_p^F in \mathcal{D}^F (fluid).

Note that there are no sources or sinks inside the storage and therefore the above heat equation appears without forcing term. Based on this assumption, the heat equation (4.2.1) can be written as

$$\frac{\partial Q}{\partial t} = d\Delta Q - v \cdot \nabla Q, \quad (t, x, y) \in (0, T] \times \mathcal{D} \setminus \mathcal{D}^J, \quad (4.5)$$

where $\Delta = \frac{\partial^2}{\partial x^2} + \frac{\partial^2}{\partial y^2}$ is the Laplace operator and $d = d(x,y)$ is the thermal diffusivity which is piecewise constant with values $d^\dagger = \frac{\kappa^\dagger}{\rho^\dagger c_p^\dagger}$ with $\dagger = M$ for $(x,y) \in \mathcal{D}^M$ and $\dagger = F$ for $(x,y) \in \mathcal{D}^F$, respectively. The initial condition $Q(0, x, y) = Q_0(x, y)$ is given by the initial temperature distribution Q_0 of the storage.

4.2.2. Boundary and Interface Conditions

For the description of the boundary conditions we decompose the boundary $\partial\mathcal{D}$ into several subsets as depicted in Fig. 4.2 representing the insulation on the top and the side, the open bottom, the inlet and outlet of the PHXs. Further, we have to specify conditions at the interface between PHXs and soil. The inlet, outlet and the interface conditions model the heating and cooling of the storage via PHXs. We distinguish between the two regimes ‘‘pump on’’ and ‘‘pump off’’, where for simplicity, we assume perfect insulation at inlet and outlet if the pump is off. Since we focus on the heat transfer over the open bottom boundary, we neglect the losses over the insulated top and side and assume perfect insulation at these boundaries. This leads to the following boundary conditions.

- *Homogeneous Neumann condition* describing perfect insulation on the top and the side

$$\frac{\partial Q}{\partial \mathbf{n}} = 0, \quad (x, y) \in \partial\mathcal{D}^T \cup \partial\mathcal{D}^L \cup \partial\mathcal{D}^R, \quad (4.6)$$

where $\partial\mathcal{D}^L = \{0\} \times [0, l_y] \setminus \partial\mathcal{D}^I$, $\partial\mathcal{D}^R = \{l_x\} \times [0, l_y] \setminus \partial\mathcal{D}^O$, $\partial\mathcal{D}^T = [0, l_x] \times \{l_y\}$ and \mathbf{n} denotes the outer-pointing normal vector.

- *Robin condition* describing heat transfer at the bottom

$$-\kappa^M \frac{\partial Q}{\partial \mathbf{n}} = \lambda^G (Q - Q^G(t)), \quad (x, y) \in \partial\mathcal{D}^B,$$

with $\partial\mathcal{D}^B = (0, l_x) \times \{0\}$, where $\lambda^G > 0$ denotes the heat transfer coefficient and $Q^G(t)$ the underground temperature.

- *Mixed boundary conditions at the inlet:* Here one has to distinguish three cases.
 - Charging:* The pump is on ($v_0 > 0$), the fluid arrives at the storage with the inlet temperature Q_C^I which is a given constant, and we can impose a Dirichlet boundary condition.
 - Waiting:* The pump is off ($v_0 = 0$), and we set a homogeneous Neumann condition describing perfect insulation.
 - Discharging:* In this mode, the pump is switched on ($v_0 > 0$) and the operation of the heat pump must be taken into account. The fluid from the PHX outlet arrives at the inlet of the heat pump with the temperature $\bar{Q}^O(t)$ and returns to the inlet of the geothermal storage at the

temperature $\bar{Q}^O(t) - \Delta T_{HP}$, where $\Delta T_{HP} > 0$ is called heat pump spread and assumed to be a given constant. Mathematically, this leads to a coupling condition which links the inlet temperature to the average temperature at the PHX outlet.

Summarizing, we obtain:

$$\begin{cases} Q = Q_C^I, & \text{charging,} \\ \frac{\partial Q}{\partial \mathbf{n}} = 0, & \text{waiting,} \\ Q = \bar{Q}^O(t) - \Delta Q_{HP}, & \text{discharging,} \end{cases} \quad (x, y) \in \partial \mathcal{D}^I. \quad (4.7)$$

- “*Do Nothing*” condition at the outlet in the following sense. If the pump is on ($v_0 > 0$), then the total heat flux directed outwards can be decomposed into a diffusive heat flux given by $\kappa^F \frac{\partial Q}{\partial \mathbf{n}}$ and a convective heat flux given by $v_0 \rho^F c_p^F Q$. In our model, we can neglect the diffusive heat flux. This leads to a homogeneous Neumann condition

$$\frac{\partial Q}{\partial \mathbf{n}} = 0, \quad (x, y) \in \partial \mathcal{D}^O.$$

If the pump is off, then we assume perfect insulation which is also described by the above condition.

- *Smooth heat flux* at interface \mathcal{D}^J between fluid and soil leading to a coupling condition

$$\kappa^F \frac{\partial Q^F}{\partial \mathbf{n}} = \kappa^M \frac{\partial Q^M}{\partial \mathbf{n}}, \quad (x, y) \in \mathcal{D}^J. \quad (4.8)$$

Here, Q^F, Q^M denote the temperature of the fluid inside the PHX and of the soil outside the PHX, respectively. Moreover, we assume that the contact between the PHX and the medium is perfect which leads to a smooth transition of a temperature, that is, we have

$$Q^F = Q^M, \quad (x, y) \in \mathcal{D}^J. \quad (4.9)$$

4.2.3. Aggregated Characteristics

The solution of the heat equation (4.5) allows to describe the spatio-temporal temperature distribution in the GES. However, for the optimal management of a residential heating system equipped with a GES, which we consider in this article, it is not necessary to know the complete information about this distribution, that is, $Q(t, x, y)$ at each individual grid point. Instead, it is sufficient to know only the dynamics of some aggregated quantities of the temperature distribution, e.g. the average temperature in the storage medium, in the PHX and at the outlet boundary of the PHX. They can be computed by post-processing after solving the PDE. Some of these aggregated characteristics are presented below. We start with the average temperature in the medium and the fluid. They are given by

$$\bar{Q}^\dagger(t) = \frac{1}{|\mathcal{D}^\dagger|} \iint_{\mathcal{D}^\dagger} Q(t, x, y) dx dy, \quad \dagger = M, F,$$

where $\bar{Q}^M(t)$ denotes the average temperature in the medium and \bar{Q}^F the average temperature of the fluid of the PHXs. These quantities allow to determine the amount of thermal energy stored. Below in

Subsect. 6.2, we will require that \bar{Q}^M satisfies the state constraint $\bar{Q}^M(t) \in [\underline{q}, \bar{q}]$ for all $t \in [0, T]$ with $\underline{q} < \bar{q}$, which leads to a state-dependent control constraint.

Another aggregated characteristics is the average temperature at the outlet boundary given by

$$\bar{Q}^O(t) = \frac{1}{|\partial\mathcal{D}^O|} \int_{\partial\mathcal{D}^O} Q(t, x, y) ds. \quad (4.10)$$

We refer to [30] and [31, Section 5] for more details.

4.3. Average Temperature in the Internal Storage

The IES is assumed to be a stratified water tank. For the ease of exposition we assume that the technical implementation is such that there is a constant and known bottom temperature \underline{p} and top temperature $\bar{p} > \underline{p}$. Further, we only consider the spatially averaged temperature of the IES as state variable, which we denote by P .

We assume that charging the GES by transferring heat from the IES is such that a (conventional) pump sends fluid with an inlet temperature Q_C^I from the IES to the GES. After passing the GES the fluid returns to the IES with the GES outlet temperature $\bar{Q}^O(t)$. Charging the IES by transferring heat from the GES is such that heat pump raises the temperature of the fluid from P_{out} , to a given constant and known temperature P_{in} with $P_{in} > \underline{p}$. In this process, the heat pump uses the heat extracted from the GES and additional electrical energy. More details about charging and discharging processes are given in Sect. 2

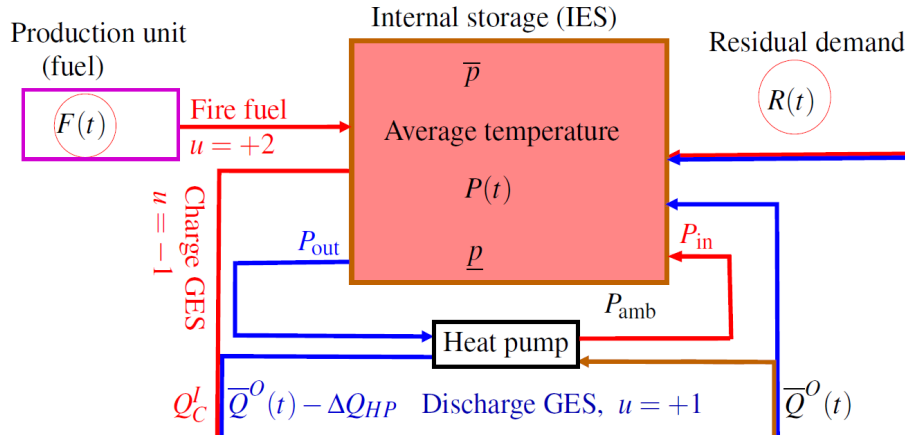


Figure 4.3. Changes of thermal energy in the internal storage

The changes of thermal energy in the IES are either due to inflow of energy from overproduction, or from the GES, or by firing fuel. Further, there may be an outflow of energy to satisfy the positive residual demand, or to the GES, or due to the loss to environment as depicted in Fig. 4.3. The environment is assumed to be at temperature $P_{amb}(t) < \underline{p}$ which may vary over time. The dynamics of the IES is then given by

$$dP(t) = (\eta_P(t, R(t), \bar{Q}^O(t), u(t)) - \gamma(P(t) - P_{amb}(t)))dt, P(0) = p_0 \in [\underline{p}, \bar{p}], \quad (4.11)$$

where R is the deseasonalized residual demand given by equation (4.2) and \bar{Q}^O is the average temperature of the fluid at the outlet of the PHXs given in (4.10). The quantity $-\gamma(P - P_{amb})$ is the heat loss

to the environment at time t , where $\gamma = \kappa^P A^P / (m^P c_p^W)$ is a constant with m^P the mass of the water in the IES, c_p^W the specific heat capacity of the water, κ^P the heat transfer coefficient, A^P the total surface of the IES. The function η_P is given by

$$\eta_P(t, r, q, a) = \begin{cases} -\zeta_P(\mu_R(t) + r) + \zeta_F, & a = +2, \\ -\zeta_P(\mu_R(t) + r) + \zeta_C(P_{\text{in}} - P_{\text{out}}), & a = +1, \\ -\zeta_P(\mu_R(t) + r), & a = 0, \\ -\zeta_P(\mu_R(t) + r) - \zeta_D(Q_C^I - q), & a = -1, \\ 0, & a = -2, \end{cases} \quad (4.12)$$

for $t \in [0, T]$, $r \in \mathbb{R}$, $q \in [q, \bar{q}]$, $a \in \mathcal{K}$. Here, $\zeta_P = (m^P c_p^W)^{-1}$, $\zeta_D = \zeta_P L_D$, $\zeta_C = \zeta_P L_C$, and $\zeta_F = \zeta_P L_F$ are energy conversion factors with some positive constants L_D , L_C , L_F . The increment of the total thermal energy in the IES at time t is then given by $m^P c_p^W dP(t)$. In the dynamics of the IES we assume that $P_{\text{in}} > P_{\text{out}}$. The residual demand $\tilde{r} = \mu_R(t) + r$ appears in the dynamics of P with negative sign because a positive residual demand decreases the temperature in the IES and a negative residual demand increases temperature in the IES. Note that during over-spilling ($a = -2$) the ODE (4.11) for P reads $dP = -\gamma(P - P_{\text{amb}})dt$. It describes the cooling of IES by the colder environment. For simplicity, any other inflows and outflows of energy are neglected by setting $\eta_P = 0$. This will facilitate the time discretization below in Subsect. 6.1 and the construction of a transition operator with additive Gaussian noise in Proposition 6.3.

Below in Subsect. 6.2, we will require that P satisfies the state constraint $P(t) \in [p, \bar{p}]$ for all $t \in [0, T]$ which leads to a state-dependent control constraint. Note that (4.11) is a random ODE, since the drift coefficient depends on the stochastic process R . In contrast to an SDE, it does not contain a diffusion term and is not driven by a Wiener process.

5. Approximation of State Dynamics

We recall that the dynamics of R and F are given by the SDEs (4.2) and (4.4), and P is governed by the random ODE (4.11). The state Q , the temperature distribution in the GES, is governed the initial boundary value problem for the linear parabolic PDE (4.5)

$$\frac{\partial}{\partial t} Q(t, x, y) = d(x, y) \Delta Q(t, x, y) - v(t, x, y) \cdot \nabla Q(t, x, y), \quad (t, x, y) \in (0, T] \times \mathcal{D} \setminus \mathcal{D}^J,$$

$$Q(0, x, y) = Q_0, \quad (x, y) \in \mathcal{D}$$

+ boundary and interface conditions given in (4.6) through (4.9).

Giving that one of the state components, the temperature $Q = Q(t, x, y)$ in the GES, depends not only on time t but also on spatial variables and its dynamics is governed by a PDE, the state process $X = (R, F, P, Q)'$ takes values in an infinite-dimensional space. This leads to a *non-standard* stochastic optimal control problem for which we do not expect to find a tractable solution. We therefore consider the following finite-dimensional approximation.

Approximation of the temperature distribution in the GES. A detailed inspection of the control system, and in particular the state and control constraints in Subsect. 6.5 and the associated performance criterion in Subsect. 6.2 show that, we do not really need to know the complete spatio-temporal

temperatures distribution. As already outlined in Subsection 4.2.3, where we introduced aggregated quantities of the temperature distribution, it is sufficient to know only the dynamics of the average temperature in the storage medium, in the PHX and at the outlet boundary of the PHX, which we denote by $\bar{Q}^M, \bar{Q}^F, \bar{Q}^O$, respectively. Let $\bar{Z} : [0, T] \rightarrow \mathbb{R}^{n_O}$ denote vector function containing as entries the desired above mentioned aggregated characteristics describing the dynamics of the spatial temperature distribution in the GES. We denote by \bar{Z} the output variable. A typical example for $n_O = 3$ is $\bar{Z} = (\bar{Q}^M, \bar{Q}^F, \bar{Q}^O)'$.

In the previous work [29], we have shown that by applying model order reduction techniques to the spatially discretized heat equation 4.5, one can find quite accurate approximations of the dynamics of the output \bar{Z} from a suitable chosen low-dimensional system of ODEs. We only briefly outline the corresponding approximation steps here.

- (i) The first step is to approximate the original mathematical model given by the PDE (4.5), by an “analogous model” with time-invariant dynamics. We assume that, in contrast to the original model, the fluid always moves at a constant velocity \bar{v}_0 , even during the pump-off periods. During these periods, the fluid in the original model is at rest and is only subject to diffusive heat propagation. In order to imitate this behaviour of the fluid at rest by a moving fluid, we assume that the temperature at the inlet of the PHX is equal to the average temperature of the PHX fluid \bar{Q}^F . In this way, the average temperature of the fluid is maintained. Approximation errors may occur, as a possible temperature gradient along the PHX is not maintained and is replaced by an almost flat temperature distribution.

Mathematically, in this setting, the initial boundary value problem for the heat equation (4.5) now contains a modified boundary condition at the inlet. During pump-off periods, the homogeneous Neumann boundary condition in (4.7) is replaced by a nonlocal coupling condition similar the condition we already impose during discharging the GES. For further details, we refer to our work [29, Section 5].

- (ii) The next step is a spatial discretization of the initial boundary value problem for the PDE (4.5) for Q , modified as described above. Following our previous work [31], this leads to a system of ODEs for a vector function $\tilde{Y} : [0, T] \rightarrow \mathbb{R}^n$ with a high dimension n . For a finite difference discretization as in [31], the entries $\tilde{Y}_i(t)$ represent the temperature at the i -th grid point. The desired aggregated characteristics, that is, the entries of the output \bar{Z} , can be approximated by linear combinations of the entries of the \tilde{Y} . Mathematically, this can be expressed as $\bar{Z}(t) \approx \tilde{Z}(t) = \tilde{C}\tilde{Y}(t)$, where $\tilde{Z} \in \mathbb{R}^{n_O}$ denotes the output approximation, and \tilde{C} an $n_O \times n$ matrix.
- (iii) Finally, we apply balanced truncation model order reduction as presented in [29, Section 6] to the resulting n -dimensional system of ODEs. This leads to a system of ODEs of dimension $\ell \ll n$ for an ℓ -dimensional reduced-order state Y from which approximations of the output variables are obtained by linear combination of the entries of Y , that is, $Z(t) \approx \bar{Z}(t) = CY(t)$, where C is a $n_O \times \ell$ matrix. For the above mentioned example with $n_O = 3$ and output $\bar{Z} = (\bar{Q}^M, \bar{Q}^F, \bar{Q}^O)'$, we find the approximations of the form $\bar{Q}^\dagger \approx Q^\dagger = C^\dagger Y(t)$, $\dagger = M, F, O$, where the n_O -dimensional vectors C^\dagger form the rows of the matrix $C \in \mathbb{R}^{3 \times \ell}$.

To summarise, the dynamics of the GES and the response of the aggregated characteristics to the

control process $u(t)$ can be represented approximately as follows

$$\begin{aligned} dY(t) &= \eta_Y(t, Y(t), u(t))dt, & Y(0) &= y_0 \in \mathbb{R}^\ell, \\ Z(t) &= CY(t), \end{aligned} \quad (5.1)$$

where $\eta_Y(t, y, a) = A(a)y + Bg(t, a)$ for $a \in \mathcal{K}$, $y = (y^1, \dots, y^\ell)' \in \mathbb{R}^\ell$ denotes the reduced-order state, and y_0 its initial value at time $t = 0$. The second equation in (5.1) is an algebraic equation called output equation in which C is the $n_O \times \ell$ -output-matrix introduced above. Its entries depend on the type of information the manager wishes to get from the system, and $Z \in \mathbb{R}^{n_O}$ is the vector of approximated aggregated characteristics. The control-dependent system matrix $A(a)$ is given by (see [28, Section 5.1])

$$A(a) = \begin{cases} \bar{A}, & a = -1 \text{ (charge GES)}, \\ \bar{A} + B^1 C^O, & a = +1 \text{ (discharge GES)}, \\ \bar{A} + B^1 C^F, & \text{otherwise,} \end{cases} \quad (5.2)$$

with $\bar{A} \in \mathbb{R}^{\ell \times \ell}$ and $B = (B^1, B^2) \in \mathbb{R}^{\ell \times 2}$ is the input matrix, resulting from the application of balanced truncation model order reduction. The input function g is given by

$$g(t, a) = \begin{pmatrix} Q_a^I(t) \\ Q_G(t) \end{pmatrix} \text{ with } Q_a^I(t) = \begin{cases} Q_C^I, & a = -1 \text{ (charge GES)}, \\ -\Delta_{\text{HP}}, & a = +1 \text{ (discharge GES)}, \\ 0, & \text{else.} \end{cases} \quad (5.3)$$

Recall, Q_C^I is the GES inlet temperature during charging, Δ_{HP} the heat pump spread, and $Q_G(t)$ the underground temperature.

Approximated state dynamics. Now, we are able to approximate the dynamics of the infinite dimensional state $(R, F, P, Q)'$ by the dynamics of a finite-dimensional state $X = (R, F, P, Y)'$ taking values in a state space $\mathcal{X} \subset \mathbb{R}^{\ell+3}$, where ℓ denotes the dimension of the vector function Y which replaces and approximates the last state component, the spatial temperature distribution Q . The continuous-time dynamics of this state process X is given by the SDE (4.2) for the residual demand R , the SDE (4.4) for fuel price F , the random ODE (4.11) for P , the average temperature in the IES, and finally, the ℓ -dimensional system of ODEs (5.1) for Y .

Remark 5.1. *In such a continuous-time setting, the cost-optimal management of a residential heating system with a GES can be formulated as an optimization problem for a (degenerate) controlled diffusion process. Applying the standard dynamic programming solution approach results in the Hamilton-Jacobi-Bellman (HJB) equation, a highly nonlinear PDE that serves as a necessary optimality condition. Apart from various analytical problems arising from the fact that the state process is a degenerate diffusion process, this approach suffers from the curse of dimensionality. The main problem is that the HJB equation can only be solved numerically, and the computational cost of solving such nonlinear PDEs with $\ell + 3$ state variables is prohibitively high. Therefore, in the next section, we proceed with a more tractable approach based on time discretization.*

6. Stochastic Optimal Control Problem

In this section, we formulate the cost-optimal management problem for a residential heating system mathematically as a discrete-time stochastic optimal control problem. The derivation is based on a time discretization of the continuous-time state dynamics studied above. The starting point is the assumption, often fulfilled in reality, that the control can only be changed at a few discrete points in time and held constant in between. To avoid discretization errors, it is assumed that the state variables evolve continuously in time between discrete time points and are determined by the ODEs and SDEs derived in sections 4 and 5, which capture the dynamics of the system. In the derived control system, however, only the state values at the discrete points in time are used for the control decisions. The control problem is then treated as a MDP and solved using dynamic programming techniques.

6.1. Time Discretization

Recall that, the state process $X = (R, F, P, Y)'$ takes values in the state space $\mathcal{X} \subset \mathbb{R}^d$ of dimension $d = \ell + 3$, where ℓ is the dimension of the reduced-order state Y from the approximation of the GES temperature distribution, see (5.1). We subdivide the planning horizon $[0, T]$ into N uniformly spaced subintervals of length $\Delta t = T/N$ and define the time grid points $t_n = n\Delta t$ for $n = 0, \dots, N$.

Discrete-time control and state process. Now, we want to study the dynamics of the state process X sampled at the discrete time points $t_n, n = 0, \dots, N$, under the following assumption.

Assumption 6.1. (*Piecewise constant control*).

The control u is kept constant between two consecutive grid points of the time discretization, that is

$$u(t) = u(t_n) =: \alpha_n, \quad \text{for } t \in [t_n, t_{n+1}), \quad n = 0, \dots, N-1,$$

and denote by $\alpha = (\alpha_n)_{n=0, \dots, N-1}$ the sequence of controls or actions $\alpha_n \in \mathcal{K} = \{-2, +1, 0, -1, +2\}$ chosen by the decision maker in period $[t_n, t_{n+1}]$.

Next, we derive the discrete-time dynamics of the sampled state process $X = (X_n)_{n=0, \dots, N}$ in terms of a recursion. Starting point is the dynamics of the the continuous-time state process given by the SDE (4.2) for R , SDE (4.4) for F , the random ODE (4.11) for P , and the ℓ -dimensional system of ODEs (5.1) for Y . Since all these equations are linear, we can benefit from the availability of closed-form solutions that allow us to avoid discretization errors in the derivation of the discrete-time state dynamics. To simplify the calculations, we assume the following for the time-dependent model parameters.

Assumption 6.2. (*Piecewise constant model parameters*).

The time-varying seasonalities μ_R, μ_F , volatilities σ_R, σ_F , the ambient temperature P_{amb} , and the underground temperature Q^G are constant between two consecutive grid points of the time discretization, that is

$$\begin{aligned} \mu_{\dagger}(t) &= \mu_{\dagger}(t_n) = \mu_{\dagger, n}, & \sigma_{\dagger}(t) &= \sigma_{\dagger}(t_n) = \sigma_{\dagger, n}, \quad \dagger = R, F, \\ P_{amb}(t) &= P_{amb}(t_n) = P_{amb, n}, & Q^G(t) &= Q^G(t_n) = Q_n^G, \end{aligned}$$

for $t \in [t_n, t_{n+1}), \quad n = 0, \dots, N-1$.

Note that this assumption is not very restrictive, since in reality these parameters can be expected to change only slowly over time and to be nearly constant on short time scales such as the periods during which the control is held constant.

Proposition 6.3 (Transition operator). *Under Assumptions 6.1 and 6.2, there exists a sequence of independent three-dimensional standard normally distributed random vectors for $(\mathcal{B}_n)_{n=1,\dots,N}$ with $\mathcal{B}_n = (\mathcal{B}_n^R, \mathcal{B}_n^F, \mathcal{B}_n^P)' \in \mathcal{N}(0_3, \mathbb{I}_3)$ such that the state process $X = (X_n)_{n=0,\dots,N}$ satisfies the recursion*

$$X_{n+1} = \mathcal{T}(n, X_n, \alpha_n, \mathcal{B}_{n+1}), \quad X_0 = X(0) = x_0. \quad (6.1)$$

for $n = 0, \dots, N-1$. Here, $\mathcal{T} : \{0, \dots, N-1\} \times \mathcal{X} \times \mathcal{K} \times \mathbb{R}^3 \rightarrow \mathcal{X}$ is the transition operator which is for $n \in \{0, \dots, N-1\}$, $x = (r, f, p, y) \in \mathcal{X}$, $a \in \mathcal{K}$, $b = (b^R, b^F, b^P)' \in \mathbb{R}^3$ defined as $\mathcal{T} = (\mathcal{T}^R, \mathcal{T}^F, \mathcal{T}^P, (\mathcal{T}^Y)')'$ with

$$\begin{aligned} \mathcal{T}^R(n, x, a, b) &= r e^{-\beta_R \Delta_N} + \Sigma_R(n) b^R, \\ \mathcal{T}^F(n, x, a, b) &= f e^{-\beta_F \Delta_N} + \Sigma_F(n) b^F, \\ \mathcal{T}^P(n, x, a, b) &= e^{-\gamma \Delta_N} p + \mathcal{H}(n, r, y, a) + \Sigma_P(n, a) (\sqrt{1 - \rho^2(n, a)} b^P + \rho(n, a) b^R), \\ \mathcal{T}^Y(n, x, a, b) &= \overline{\mathcal{T}}^Y(n, y, a) = e^{A(a) \Delta_N} y + (e^{A(a) \Delta_N} - \mathbb{I}_\ell) A^{-1} B g_n(a), \end{aligned} \quad (6.2)$$

where \mathbb{I}_ℓ is an $\ell \times \ell$ identity matrix, $A(a), B$ are given in (5.2), the functions $\Sigma_R, \Sigma_F, \Sigma_P, \rho$ and \mathcal{H} are given in Appendix B. Further, $g_n(a) = g(t_n, a)$ denotes the constant input function in $[t_n, t_{n+1})$ with $g(t, a)$ given in (5.3).

Proof. The SDE (4.1) for R and the random ODE (4.11) for P enjoy closed-form solutions yielding that R_{n+1} and P_{n+1} can be expressed in terms of stochastic integrals with respect to Wiener process W_R with a deterministic integrand from which it can be derived that the conditional distribution of R_{n+1}, P_{n+1} given $R_n = r, P_n = p$ and $\alpha_n = a$ is bivariate Gaussian. Computing mean and the covariance matrix of this distribution leads to the given expressions. Note that $\Sigma_R^2(n)$ and $\Sigma_P^2(n)$ are the variances, and $\rho(n)$ represents the correlation coefficient of this distribution. Similarly, solving the SDE (4.4) on $[t_n, t_{n+1}]$ shows that F_{n+1} can be also expressed in terms of a stochastic integral with respect to Wiener process W_F with a deterministic integrand. This implies that the conditional distribution of F_{n+1} given $F_n = f$ is Gaussian and independent of R_{n+1}, P_{n+1} since W_R, W_F are independent. Finally, Y_{n+1} can be obtained by solving the system of linear ODEs (5.1) for $Y(t)$ on $[t_n, t_{n+1}]$ with initial value $Y_n = y$. Under the Assumptions 6.1 and 6.2, this is for each fixed control a , a system of autonomous ODEs with a constant forcing term. From the closed-form solution follows the expression for \mathcal{T}^Y . For more details, we refer to [28, Chapter 6]. \square

In view of the recursion (6.1) we can consider the sampled state process $X = (X_n)_{n=0,\dots,N}$ as a discrete-time stochastic process, which is defined on the filtered probability space $(\Omega, \mathcal{F}, \mathbb{F}, \mathbb{P})$ with the filtration $\mathbb{F} = (\mathcal{F}_n)_{n=0,\dots,N}$. Here, $\mathcal{F}_n = \sigma(\{\mathcal{B}_1, \dots, \mathcal{B}_n\})$ is the sigma-algebra generated by the first n random variables $\mathcal{B}_1, \dots, \mathcal{B}_n$ and $\mathcal{F}_0 = \{\emptyset, \Omega\}$ is the trivial σ -algebra.

Further, the recursion (6.1) for the state process X shows that the conditional distribution of the state X_{n+1} at the end of the period $[t_n, t_{n+1}]$, given the state X_n and the control α_n at the beginning of that period, is Gaussian. This property will be helpful for the formulation the control problem

as Markov decision process below in Subsect. 6.5 , and the derivation of the associated transition kernel. Note that the Gaussian distribution is degenerate since the last state component Y follows deterministic dynamics. In contrast, the conditional distribution of the first three components R, F, P is a non-degenerate three-dimensional Gaussian distribution, where F is independent of R, P .

6.2. State-Dependent Control Constraints

The residential heating system under consideration is subject to various operational constraints. A first one is a box constraint for the state component P , the IES average temperature. As already mentioned in Subsection 4.3, it is required that $P(t) \in [\underline{p}, \bar{p}]$, for all $t \in [0, T]$ with $\underline{p} < \bar{p}$, where \underline{p} and \bar{p} represent an empty and a full IES, respectively. A second condition is that the authorities only permit the operation of a GES for environmental reasons, if the GES temperature does not exceed a certain range. We model this by a box constraint to the average temperature in the medium of the form $Q^M(t) \in [\underline{q}, \bar{q}]$ with $\underline{q} < \bar{q}$, where \underline{q} and \bar{q} represent an empty and a full GES, respectively. This is sufficient, as an inhomogeneous spatial temperature distribution is averaged after some time due to the diffusive propagation of heat in the GES. Since $Q^M = C^M Y$, the above constraint requires the reduced-order state $Y(t)$ to take values in the subset $\mathcal{Y} \in \mathbb{R}^\ell$ between the two hyperplanes defined by $C^M Y = \underline{q}$ and $C^M Y = \bar{q}$ for all $t \in [0, T]$, that is in

$$\mathcal{Y} \in \mathbb{R}^\ell = \{y \in \mathbb{R}^\ell : \underline{q} \leq C^M y \leq \bar{q}\}. \quad (6.3)$$

In a model in which the controls can be continuously changed over time, such restrictions mean that charging a storage (IES or GES) is no longer permitted when the storage is full, while discharging can no longer be selected for an empty storage. However, due to Assumption 6.1, we are limited to controls that are kept constant between two consecutive points in time of the time grid. In contrast to continuous operation, this means that charging or discharging is no longer permitted when the storage is “almost” full or empty.

Therefore, for each time step $n \in \{0, 1, \dots, N-1\}$, one has to derive a subset of the set of all feasible actions \mathcal{K} given in (3.1), that contain the feasible actions available to the controller depending on the state X_n at time n . The latter should be defined in such a way that the IES and GES do not become full or empty within the next period $[t_n, t_{n+1}]$. In view of the dynamics of the state components P and Y describing the IES and GES, it is sufficient to consider the state of IES and GES at the end of the period at time t_{n+1} . This leads to the following still rather implicit definition

$$\mathcal{K}_0(n, x) = \{a \in \mathcal{K} \mid \mathcal{T}(n, x, a, \mathcal{B}_{n+1}) \text{ is such that IES and GES are not full or empty}\}$$

for $n = 0, \dots, N-1$ and $x \in \mathcal{X}$.

Now, we will show how this simple and intuitive idea can be formulated in a mathematically rigorous way. Recall, that we have from recursion (6.1), $P_{n+1} = \mathcal{T}^P(n, X_n, \alpha_n, \mathcal{B}_{n+1})$. Further, the conditional distribution of the IES temperature P_{n+1} given X_n is Gaussian. This prohibits to satisfy the box constraint $P_{n+1} \in [\underline{p}, \bar{p}]$ with certainty and requires a relaxation. Therefore, we allow over- and undershooting, that is, $P_{n+1} > \bar{p}$ and $P_{n+1} < \underline{p}$, but constrain the probabilities for these events by some “small” tolerance value $\varepsilon < 1$. Furthermore, the recursion (6.1) for P shows that, the Gaussian distribution of P_{n+1} depends on the deseasonalized residual demand R_n at time t_n . As a realization of a

Gaussian random variable, these values are potentially unbounded, making it impossible to define reasonable relaxed constraints to P_{n+1} . Note that R is an exogenous state and is not subject to control. Therefore, we restrict the following derivations to a bounded interval $[\underline{r}, \bar{r}] \subset \mathbb{R}$ with $\underline{r} < \bar{r}$ in which the random variables R_n take values with very high probability. Since the sampled continuous-time process R is a Gaussian Ornstein-Uhlenbeck process for which the marginal distribution of $R(t)$ converges asymptotically for $t \rightarrow \infty$ to the stationary distribution $\mathcal{N}(0, \sigma_R^2/(2\beta_R))$. We apply the 3σ -rule and choose $[\underline{r}, \bar{r}] = [-3\sigma_R/(2\beta_R)^{1/2}, +3\sigma_R/(2\beta_R)^{1/2}]$, which carries 99.97% of the probability mass of this distribution.

The above mentioned restrictions are formalized by the following truncation operator $\mathcal{R} : \mathcal{X} \rightarrow \mathcal{X}_{\mathcal{R}} = [\underline{r}, \bar{r}] \times [\underline{p}, \bar{p}] \times \mathbb{R}^{\ell}$, which is defined for $x = (r, p, y')' \in \mathcal{X}$ by

$$\mathcal{R}(x) = (\underline{r}\mathbb{1}_{(-\infty, \underline{r})}(r) + r\mathbb{1}_{[\underline{r}, \bar{r}]}(r) + \bar{r}\mathbb{1}_{(\bar{r}, \infty)}(r), \underline{p}\mathbb{1}_{(-\infty, \underline{p})}(p) + p\mathbb{1}_{[\underline{p}, \bar{p}]}(p) + \bar{p}\mathbb{1}_{(\bar{p}, \infty)}(p), y')',$$

where $\mathbb{1}$ denotes the indicator function. This operator maps the values of r and p outside $[\underline{r}, \bar{r}]$ and $[\underline{p}, \bar{p}]$ to the nearest boundaries of the intervals. Then the desired set of feasible actions is expressed for $n = 0, \dots, N-1$ and $x \in \mathcal{X}$ by

$$\mathcal{K}(n, x) = \mathcal{K}^P(n, x) \cap \mathcal{K}^Y(n, x), \quad \text{where} \quad (6.4)$$

$$\mathcal{K}^P(n, x) = \{a \in \mathcal{K} \mid \mathbb{P}(\mathcal{T}^P(n, \mathcal{R}(x), a, \mathcal{B}_{n+1}) > \bar{p}) \leq \varepsilon \quad \text{and} \quad \mathbb{P}(\mathcal{T}^P(n, \mathcal{R}(x), a, \mathcal{B}_{n+1}) < \underline{p}) \leq \varepsilon\}, \quad (6.5)$$

$$\mathcal{K}^Y(n, x) = \{a \in \mathcal{K} \mid C^M \overline{\mathcal{T}}^Y(n, y, a) \in [\underline{q}, \bar{q}]\}. \quad (6.6)$$

The explicit description of the above subsets describing state-dependent control constraints is based on the following assumptions to the model parameters.

Assumption 6.4.

1. For all $n = 0, \dots, N-1, x \in \mathcal{X}_{\mathcal{R}}, b \in \mathbb{R}^3$ it holds

$$\mathcal{T}^P(n, x, +2, b) > \mathcal{T}^P(n, x, +1, b) > \mathcal{T}^P(n, x, 0, b) > \mathcal{T}^P(n, x, -1, b). \quad (6.7)$$

2. For all $n = 0, \dots, N-1$ it holds that within the period $[t_n, t_{n+1}]$ a full GES cannot be completely discharged:

$$\mathcal{Y}^C(n) = \{y \in \mathcal{Y} : C^M \overline{\mathcal{T}}^Y(n, y, +1) \geq \underline{q}\} \neq \emptyset,$$

an empty GES cannot be fully charged:

$$\mathcal{Y}^D(n) = \{y \in \mathcal{Y} : C^M \overline{\mathcal{T}}^Y(n, y, -1) \leq \bar{q}\} \neq \emptyset,$$

there are states of the GES for which the action $a = 0$ (wait) is feasible

$$\mathcal{Y}^W(n) = \mathcal{Y} \setminus (\mathcal{Y}^C(n) \cup \mathcal{Y}^D(n)) \neq \emptyset.$$

3. For all $x = (r, p, y')' \in \mathcal{X}_{\mathcal{R}}$, and $n = 0, \dots, N-1$ it holds that within the period $[t_n, t_{n+1}]$ a full IES cannot be completely discharged:

$$\{p \in [\underline{p}, \bar{p}] : \mathbb{P}(\mathcal{T}^P(n, x, -1, \mathcal{B}_{n+1}) \geq \underline{p}) \geq 1 - \varepsilon\} \neq \emptyset$$

an empty IES cannot be fully charged:

$$\{p \in [\underline{p}, \bar{p}] : \mathbb{P}(\mathcal{T}^P(n, x, +2, \mathcal{B}_{n+1}) \leq \bar{p}) \geq 1 - \varepsilon\} \neq \emptyset$$

4. The lower and upper bounds for Q^M are such that the underground temperature satisfies $\underline{q} \leq Q^G(t) \leq \bar{q}$ for all $t \in [0, T]$.

Remark 6.5. The first assumption reflects a natural condition for the model parameters, which are such that for a given state x at time t_n and a realization b of the random variable \mathcal{B} , the realizations of the IES temperature at time t_{n+1} , $P_{n+1} = p$, satisfy the given order with respect to the different actions $a \in \mathcal{K}$. Thus, firing fuel leads to a higher p than the transfer of heat from GES to IES. The latter dominates waiting, and waiting leads to a higher p than the transfer of heat from IES to GES.

The second and third assumptions can always be fulfilled if the length of the time intervals Δ_N is chosen small enough. Finally, the fourth assumption states that a fully discharged GES is colder than the underground, so that a heat flow to the GES can be induced as intended, and the GES acts as a heat production unit. Furthermore, the average temperature of a full GES dominates the temperature of the underground.

Next, we describe the $\mathcal{K}^Y(n, x)$ and $\mathcal{K}^P(n, x)$ separately.

Description of the set of feasible actions $\mathcal{K}^Y(n, x)$. As already outlined above, to satisfy the box constraint to the average temperature in the GES medium $Q^M(t) = C^M Y(t) \in [\underline{q}, \bar{q}]$ for all $t \in [0, T]$, the reduced-order state $Y(t)$ has to take values in the subset $\mathcal{Y} \in \mathbb{R}^\ell$ given in (6.3). The restriction to piecewise constant controls requires to stop charging or discharging, if at a grid point $t_n, n = 0, \dots, N - 1$, the average temperature $Q_n^M = Q^M(t_n)$ is already close to \bar{q} or \underline{q} , respectively, such that it will not exceed these boundaries in the period between t_n and t_{n+1} . Using the recursion $Y_{n+1} = \bar{T}^Y(n, Y_n, a)$

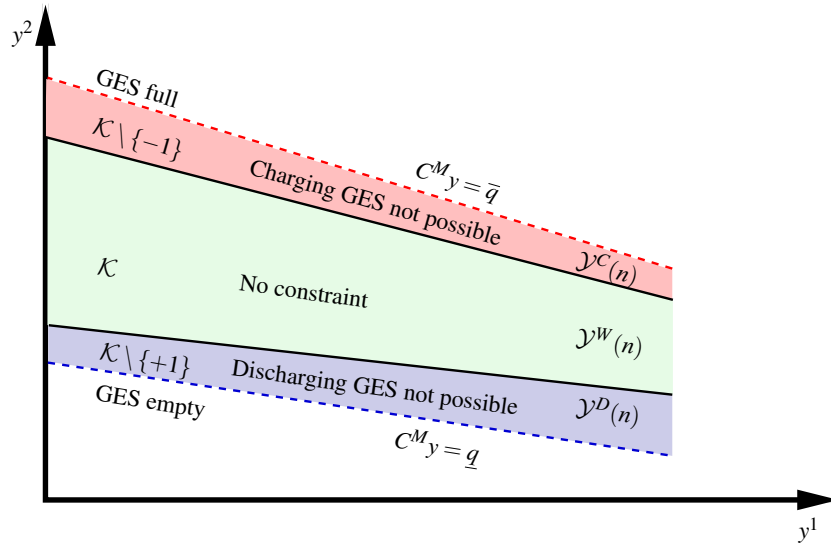


Figure 6.1. Characterization of the set of feasible control $\mathcal{K}^Y(n, x)$ for $\ell = 2$

for the sequence (Y_n) of reduced-order states given in (6.2), this leads to a decomposition of the subset \mathcal{Y} of the form $\mathcal{Y} = \mathcal{Y}^C(n) \cup \mathcal{Y}^D(n) \cup \mathcal{Y}^W(n)$ where $\mathcal{Y}^C, \mathcal{Y}^D, \mathcal{Y}^W$ are given in Assumption 6.4.2. The subsets $\mathcal{Y}^C(n)$ and $\mathcal{Y}^D(n)$ contain all states of \mathcal{Y} for which charging and discharging the GES is no longer allowed in period $[t_n, t_{n+1})$, respectively. This decomposition is sketched for the case $\ell = 2$ in

Figure 6.1. The set $\mathcal{K}^Y(n, x)$ of feasible actions introduced in (6.6) is then given for $x = (r, f, p, y)$ as

$$\mathcal{K}^Y(n, x) = \begin{cases} \mathcal{K} \setminus \{-1\}, & \text{for } y \in \mathcal{Y}^C(n), \\ \mathcal{K} \setminus \{+1\}, & \text{for } y \in \mathcal{Y}^D(n), \\ \mathcal{K}, & \text{for } y \in \mathcal{Y}^W(n). \end{cases} \quad (6.8)$$

Note that under Assumption 6.4 the above subsets $\mathcal{Y}^W(n)$ are non-empty for all $n = \dots, N-1$.

Description of the set of feasible actions $\mathcal{K}_P(n, x)$. We denote the probabilities appearing in the definition of $\mathcal{K}_P(n, x)$ in (6.5) by

$$\bar{\pi}^a(n, x) = \mathbb{P}(\mathcal{T}^P(n, \mathcal{R}(x), a, \mathcal{B}_{n+1}) > \bar{p}), \quad \text{and} \quad \underline{\pi}^a(n, x) = \mathbb{P}(\mathcal{T}^P(n, \mathcal{R}(x), a, \mathcal{B}_{n+1}) < \underline{p}),$$

which can also be interpreted as the conditional probabilities that the average IES temperature P_{n+1} at the end of the period $[t_n, t_{n+1}]$ exceeds the boundaries \underline{p}, \bar{p} if at the beginning of the period, at time t_n , the state is $X_n = x$ and the action $\alpha_n = a$ is selected.

In view of the inequalities (6.7) given in Assumption 6.4, the following monotonicity properties of $\underline{\pi}^a$ and $\bar{\pi}^a$ hold for all (n, x)

$$\bar{\pi}^{+2} > \bar{\pi}^{+1} > \bar{\pi}^0 > \bar{\pi}^{-1} \quad \text{and} \quad \underline{\pi}^{+2} < \underline{\pi}^{+1} < \underline{\pi}^0 < \underline{\pi}^{-1}.$$

Let us define the following subsets of the state space \mathcal{X} by

$$\bar{\mathcal{X}}_P^a(n) = \{x \in \mathcal{X} \mid \bar{\pi}^a(n, \mathcal{R}(x)) \leq \varepsilon\} \quad \text{and} \quad \underline{\mathcal{X}}_P^a(n) = \{x \in \mathcal{X} \mid \underline{\pi}^a(n, \mathcal{R}(x)) \leq \varepsilon\}.$$

Then for a given state $X_n = x$ at time $t = t_n$, an action $\alpha_n = a$ is feasible with respect to the constraints to P given in (6.5) if $x \in \bar{\mathcal{X}}_P^a(n) \cap \underline{\mathcal{X}}_P^a(n)$. Thus, the set of feasible controls \mathcal{K}_P can be expressed as

$$\mathcal{K}_P(n, x) = \bigcup_{a: x \in \bar{\mathcal{X}}_P^a(n) \cap \underline{\mathcal{X}}_P^a(n)} \{a\},$$

and contains those actions a for which x is in the above mentioned intersection. In view of our model setting and the dynamics of the state process, it can be deduced that the projections of the above subsets onto the sub-state spaces $\mathcal{X}_{RP} = \{(r, p) \mid x = (r, f, p, y) \in \mathcal{X}\}$, have the following form

$$\bar{\mathcal{X}}_{RP}^a(n) = \{(r, p) \mid p \leq \bar{h}_n^a(r, y)\}, \quad \text{and} \quad \underline{\mathcal{X}}_{RP}^a(n) = \{(r, p) \mid p \geq \underline{h}_n^a(r, y)\},$$

for some continuous functions $\bar{h}_n^a, \underline{h}_n^a : \mathbb{R} \times \mathbb{R}^\ell \rightarrow \mathbb{R}$ which are sketched in Fig. 6.2. Note that only for $a = -1$ there is dependence of the functions $\bar{h}_n^a, \underline{h}_n^a$ on the variable y since during discharging the IES its average temperature P depends on the outlet temperature $Q^O = C^O Y$ of the GES, see (4.11) and (4.12). It follows, that the set $\mathcal{K}_P(n, x)$ can be subdivided into 8 subsets, which follow from a decomposition of the state space \mathcal{X}_{RP} for the pair of state components (R, P) , which is depicted in Fig 6.3.

6.3. Performance Criterion

We now want to describe the costs arising in the operation of the residential heating system and derive a performance criterion for the optimization problem. This criterion summarises the expected

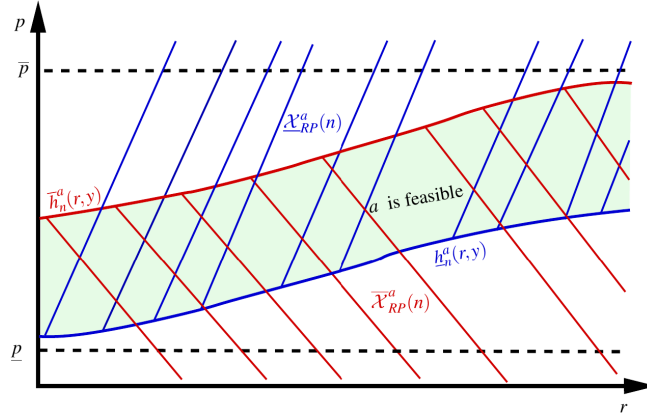


Figure 6.2. Projection of $\underline{\mathcal{X}}_P^a(n)$ and $\overline{\mathcal{X}}_P^a(n)$ onto \mathcal{X}_{RP}

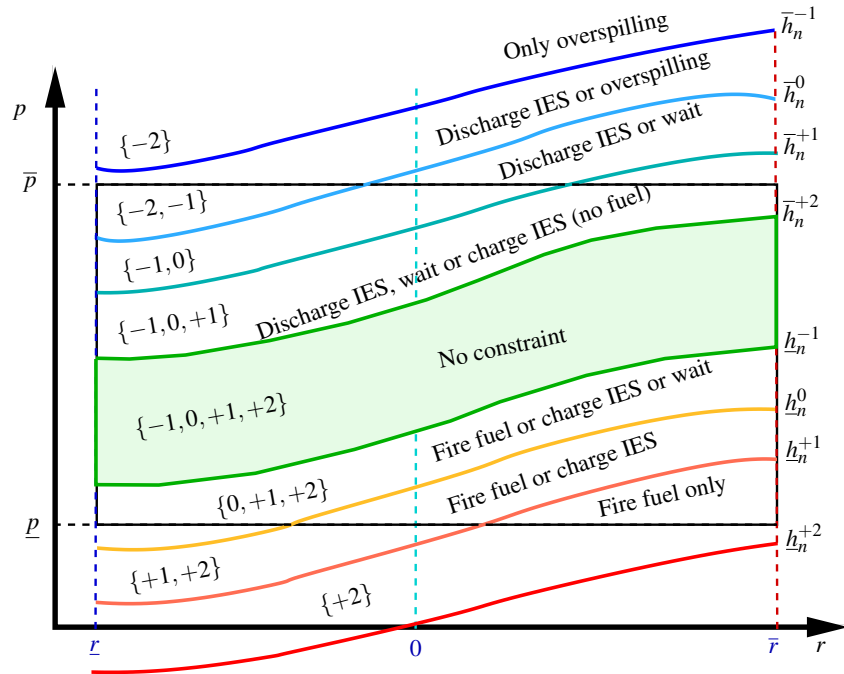


Figure 6.3. Projection of the set of feasible controls $\mathcal{K}_P(n,x)$ onto \mathcal{X}_{RP}

total discounted costs from the operation of the system and the expected discounted terminal costs from the evaluation of the stored thermal energy in the IES and GES.

Admissible controls. We denote by \mathcal{A} the set of admissible controls $\alpha = (\alpha_0, \dots, \alpha_{N-1})$ for which, we want to define below the performance criterion that will be minimized within this set. Since we want to apply dynamic programming methods for solving the optimization problem, we restrict ourselves to Markov or feedback controls defined by $\alpha_n = \tilde{\alpha}(n,x)$ with a measurable function $\tilde{\alpha} : \{0, \dots, N-1\} \times \mathcal{X} \rightarrow \mathcal{K}$ which is called *decision rule*. Note that such Markov controls α are by construction adapted to the filtration \mathbb{F} . Taking into account the state-dependent control constraints derived in Subsect. 6.2

the set of admissible controls is given by

$$\mathcal{A} = \left\{ \alpha = (\alpha_0, \dots, \alpha_{N-1}) \mid \alpha \text{ is a Markov control with } \alpha_n = \tilde{\alpha}(n, X_n^\alpha) \text{ for all } n = 0, \dots, N-1, \right. \\ \left. \text{and } \tilde{\alpha}(n, x) \in \mathcal{K}(n, x) \text{ for all } (n, x) \in \{0, 1, \dots, N-1\} \times \mathcal{X} \right\}. \quad (6.9)$$

Continuous-time performance criterion. Let us identify the sequence $\alpha = (\alpha_n)_{n=0, \dots, N-1}$ defining an admissible discrete-time control process with the piecewise constant continuous-time control $\bar{u}(t) = \sum_{n=0}^{N-1} \alpha_n \mathbb{1}_{[t_n, t_{n+1})}(t)$, see Assumption 6.1. Then, given the continuous-time state process $X = X^{\bar{u}} = (X^{\bar{u}}(t))_{t \in [0, T]}$ starts at initial time at $X^{\bar{u}}(0) = x_0 \in \mathcal{X}$, the performance of an admissible control $\alpha \in \mathcal{A}$ is given by

$$\mathcal{J}_0(x_0; \alpha) = \mathbb{E} \left[\int_0^T e^{-\delta s} \psi(X^{\bar{u}}(s), \bar{u}(s)) ds + e^{-\delta T} \phi_N(X^{\bar{u}}(T)) \right] \quad (6.10)$$

where $\delta \geq 0$ denotes the discount factor, and ψ and ϕ_N denote the running and terminal costs, respectively, which we specify below. Working with discounted costs takes into account the fact that a GES is designed to store thermal energy over longer periods of time (many weeks and months instead of days). Therefore, the economic evaluation should also take into account the time value of money expressed by the discount factor $e^{-\delta s}$.

Running costs. These costs rates measured in monetary unites per unit of time, which are defined by

$$\psi(x, a) = \begin{cases} \xi_F f, & a = +2, \\ \xi_{HP}(P_{\text{in}} - C^O y) + \xi_P, & a = +1, \\ \xi_P, & a = -1, \\ 0, & a = \{0, -2\}. \end{cases}$$

Here, ξ_F is the fuel consumption rate of the fuel-fired boiler, ξ_{HP} the price of electricity per unit of time consumed by the heat pump to increase the temperature by $1K$, and ξ_P the price of electricity per unit of time consumed by the pumps moving the fluid between IES and GES.

Terminal costs. At the end of the planning period, a terminal cost function $\phi_N : \mathcal{X} \rightarrow \mathbb{R}$ can be used to evaluate the terminal state of the system, in particular the amount of thermal energy stored in the IES and GES, in monetary terms. A typical example are *penalty and liquidation payments* that are applied if the IES temperature P_N and the average temperatures in the GES medium $Q_N^M = C^M Y_N$ are below or above a certain user-defined critical value $p_{\text{ref}} \in [\underline{p}, \bar{p}]$ and $q_{\text{ref}} \in [\underline{q}, \bar{q}]$, respectively. Suppose that the terminal state is $X_N = x = (r, f, p, y)'$, then the terminal cost is defined by

$$\phi_N(x) = m^Q c_p^M \left(\xi_{\text{pen}}^Q (Q_N^M - q_{\text{ref}})^- - \xi_{\text{liq}}^Q (Q_N^M - q_{\text{ref}})^+ \right) + m^P c_p^F \left(\xi_{\text{pen}}^P (P_N - p_{\text{ref}})^- - \xi_{\text{liq}}^P (P_N - p_{\text{ref}})^+ \right) \quad (6.11)$$

Note that $m^Q c_p^M (Q_N^M - q_{\text{ref}})$ and $m^P c_p^F (P_N - p_{\text{ref}})$ describe the amount of thermal energy required to adjust the average temperature in the GES medium from Q_N^M to q_{ref} and the average IES temperature from P_N to p_{ref} , respectively. If these quantities are negative, a penalty is due at a fixed price $\xi_{\text{pen}}^\dagger \geq 0$, $\dagger = P, Q$, per unit of energy, which is added to the total operating costs. Conversely, if the quantity

is positive, a revenue for the liquidation of the residual energy at a fixed price $\xi_{\text{liq}}^\dagger \geq 0$ per unit of energy reduces the total costs at terminal time. The terminal cost function given in (6.11) includes the special cases of (i) only penalty payments for $\xi_{\text{pen}}^\dagger > 0, \xi_{\text{liq}}^\dagger = 0$, (ii) only liquidation revenues for $\xi_{\text{pen}}^\dagger = 0, \xi_{\text{liq}}^\dagger > 0$, and (iii) zero terminal costs for $\xi_{\text{pen}}^\dagger = \xi_{\text{liq}}^\dagger = 0, \dagger = P, Q$. An example for the choice of the critical values are the initial average temperatures in IES and GES which follow from (4.11) and (5.1), that is $p_{\text{ref}} = P_0 = p_0$ and $q_{\text{ref}} = Q_0^M = C^M y_0$. In that case, (6.11) can be used to value the storage facilities at horizon time T , which can be required if the management of the residential heating system is transferred to a new owner.

Discrete-time performance criterion. The performance criterion $\mathcal{J}_0(x_0; \alpha)$ given in (6.10) can be rewritten in terms of the sequence of values $(X_n^\alpha)_{n=0, \dots, N}$ obtained from sampling the continuous-time state process $(X^{\bar{u}}(t))_{t \in [0, T]}$. Since $(X^{\bar{u}}(t))$ is defined as solution of a system SDEs and ODEs, and admissible controls are of Markov or feedback type, the state process is a Markov process. This and an application of the tower property of conditional expectation yields

$$\begin{aligned} \mathcal{J}_0(x_0; \alpha) &= \mathbb{E} \left[\sum_{k=0}^{N-1} \mathbb{E} \left[\int_{t_k}^{t_{k+1}} e^{-\delta s} \psi(X^{\bar{u}}(s), \bar{u}(s)) ds \middle| \mathcal{F}_{t_k} \right] + e^{-\delta T} \phi_N(X_N^\alpha) \right] \\ &= \mathbb{E} \left[\sum_{k=0}^{N-1} \Psi(k, X_k^\alpha, \alpha_k) + \Phi_N(X_N^\alpha) \right], \end{aligned} \quad (6.12)$$

where for $k = 0, \dots, N-1, x \in \mathcal{X}$ and $a \in \mathcal{K}$

$$\Psi(k, x, a) = \mathbb{E}_{k,x} \left[\int_{t_k}^{t_{k+1}} e^{-\delta s} \psi(X^{\bar{u}}(s), a) ds \right] \quad \text{and} \quad \Phi_N(x) = e^{-\delta T} \phi_N(x). \quad (6.13)$$

Here, $\mathbb{E}_{k,x}(\cdot) = \mathbb{E}(\cdot | X_k = x)$ denotes the conditional expectation given that at time t_k the state is $X_k = x$.

One-period running costs. The next lemma shows that the conditional expectation appearing in the definition of the one-period running costs $\Psi(k, x, a)$ in (6.13) can be given in closed-form. Hence, the transition from the continuous-time to discrete-time setting does not suffer from additional discretization errors.

Lemma 6.6. *The one-period running costs $\Psi(k, x, a)$ defined in (6.13) are given for $k = 0, \dots, N-1, x = (r, f, p, y)' \in \mathcal{X}, a \in \mathcal{K}$, and $\delta > 0$ by $\Psi(k, x, a) = e^{-\delta k \Delta_N} \bar{\Psi}(k, x, a)$ with*

$$\bar{\Psi}(k, x, a) = \begin{cases} \frac{\xi_F \mu_{F,k}}{\delta} (1 - e^{-\delta \Delta_N}) + \frac{\xi_F f}{\delta + \beta_F} (1 - e^{-(\delta + \beta_F) \Delta_N}), & a = +2, \\ \frac{(\xi_{HP} P_{in} + \xi_P)}{\delta} (1 - e^{-\delta \Delta_N}) - \xi_{HP} C^O \left\{ (e^{(A - \delta \mathbb{I}_\ell) \Delta_N} - \mathbb{I}_\ell) (A - \delta \mathbb{I}_\ell)^{-1} y \right. \\ \left. + \left[(e^{(A - \delta \mathbb{I}_\ell) \Delta_N} - \mathbb{I}_\ell) (A - \delta \mathbb{I}_\ell)^{-1} - \frac{1}{\delta} (1 - e^{-\delta \Delta_N}) \mathbb{I}_\ell \right] A^{-1} B g_k(+1) \right\}, & a = +1, \\ \frac{\xi_P}{\delta} (1 - e^{-\delta \Delta_N}), & a = -1, \\ 0, & a = \{0, -2\}. \end{cases}$$

The proof of this Lemma is available in Appendix C.

Remark 6.7. *The non-discounted case, that is $\delta = 0$, is obtained by passing to the limit $\delta \rightarrow 0$ and using that $(1 - e^{-\delta \Delta_N})/\delta \rightarrow \Delta_N$.*

6.4. Optimization Problem

The aim of the residential heating system's manager is to find an admissible control process α defined by the associated decision rule $\tilde{\alpha}$ that minimizes the expected total discounted costs arising from the operation of the system and the evaluation of the stored thermal energy in IES and GES at terminal time. These costs have been derived in the above subsection and are given by the performance criterion $\mathcal{J}_0(x_0; \alpha)$ in (6.12). Thus, the optimization problem reads

$$\mathcal{V}_0(x_0) = \inf_{\alpha \in \mathcal{A}} \mathcal{J}_0(x_0; \alpha) \quad (6.14)$$

with \mathcal{A} given in (6.9). We call $\mathcal{V}_0(x_0)$ the *value function* of the problem. It represents the minimum expected costs described by the performance criterion.

6.5. Markov Decision Process

To solve the optimal control problem (6.14) we will apply the dynamic programming approach using MDP theory. This requires to embed (6.14) into a family of optimization problems with variable initial time $n = 0, \dots, N$ and initial state $X_n = x \in \mathcal{X}$. For each of these problems we define the performance of an admissible control $\alpha \in \mathcal{A}$ and the value function as

$$J(n, x; \alpha) = \mathbb{E}_{n, x} \left[\sum_{k=n}^{N-1} \Psi(k, X_k^\alpha, \alpha_k) + \Phi_N(X_N^\alpha) \right] \quad \text{and} \quad V(n, x) = \inf_{\alpha \in \mathcal{A}} J(n, x; \alpha). \quad (6.15)$$

A control $\alpha^* = (\alpha_0^*, \dots, \alpha_{N-1}^*) \in \mathcal{A}$ is called *optimal control* if $V(n, x) = J(n, x; \alpha^*)$ for all $n = 0, \dots, N$ and $x \in \mathcal{X}$. The associated decision rule $\tilde{\alpha}^* = \tilde{\alpha}^*(n, x)$ defining α^* is called *optimal decision rule*.

The control problem in (6.15) is a MDP with finite time horizon N , an $\ell + 3$ -dimensional state process X with dynamics given by the recursion (6.1) which reads $X_{n+1} = \mathcal{T}(n, X_n, \alpha_n, \mathcal{B}_{n+1})$, $X_0 = X(0) = x_0$. It is driven by a sequence of independent three-dimensional standard normally distributed random vectors $(\mathcal{B}_n)_{n=1, \dots, N}$ that appear in the recursion as additive noise. Thus the transition kernel of the MDP describing the conditional distribution of X_{n+1} given X_n and α_n , is given by a multivariate Gaussian distribution. The transition operator \mathcal{T} is linear in the state variable, and the control takes values in the finite action space $\mathcal{K} = \{-2, -1, 0, +1, +2\}$ and is subject to state-dependent control constraints described by the family of subsets $\mathcal{K}(n, x) \subset \mathcal{K}$ given in (6.4).

Dynamic programming equation. Solving the control problem in (6.15) is based on the Bellman principle which provides the following necessary optimality condition called Bellman equation, and constitutes a backward recursion for the value function and the the optimal decision rule. We refer to Bäuerle and Rieder [3], Puterman [23], Hernández-Lerma and Lasserre [14], and the references therein for more details in the MDP theory.

Theorem 6.8. (*Bellman equation*) *The value function V satisfies for all $x \in \mathcal{X}$*

$$\begin{aligned} V(N, x) &= \Phi_N(x), \\ V(n, x) &= \min_{a \in \mathcal{K}(n, x)} \left\{ \Psi(n, x, a) + \mathbb{E} [V(n+1, \mathcal{T}(n, x, a, \mathcal{B}_{n+1}))] \right\}, \quad n = N-1, \dots, 0. \end{aligned} \quad (6.16)$$

The optimal decision rule $\tilde{\alpha}^$ is given by the minimizer in (6.16), that is*

$$\tilde{\alpha}^*(n, x) = \operatorname{argmin}_{a \in \mathcal{K}(n, x)} \left\{ \Psi(n, x, a) + \mathbb{E} [V(n+1, \mathcal{T}(n, x, a, \mathcal{B}_{n+1}))] \right\}. \quad (6.17)$$

The dynamic programming equation (6.16) can be solved by backward recursion starting at the terminal time N . Further details can be found in [28, Chapter 6].

Remark 6.9. *Note that the controlled state process is defined by a linear recursion with additive Gaussian noise. Further, the action space \mathcal{K} is finite. Hence, the expectation defining the performance criterion of the finite horizon control problem (6.15) is bounded for all admissible controls $\alpha \in \mathcal{A}$, and the infimum over α is attained. Therefore the pointwise optimization problem in the Bellman equation (6.16) is formulated with the minimum. Further, this also allows the application of a verification theorem as in Bäuerle and Rieder [3, p. 21-23], which ensures that the solution of the Bellman equation is indeed the value function and that $\tilde{\alpha}^*$ in (6.17) is optimal.*

7. State Discretization

The challenge of the direct implementation of the backward recursion algorithm following from the Bellman equation in Theorem 6.8 is that it becomes computationally intractable due to the curse of dimensionality. On the one hand, the dimension $d = \ell + 3$ of the state space is already for moderate dimensions ℓ of the reduced-order system (5.1) quite high. Note that the choice of ℓ determines the quality of the approximation of aggregated characteristics such as Q^M, Q^O appearing in the transition operator and the control constraints. On the other hand, due to the state-dependent control constraints, no closed-form expressions for the expectation $\mathbb{E}[V(n+1, \mathcal{T}(n, x, a, \mathcal{B}_{n+1}))]$, which appear in the Bellman equation (6.16), can be expected.

To overcome these problems, we propose a computationally tractable approximation of these expectations based on a state discretization, which we describe below. For the sake of simplicity, we restrict ourselves to a model with a deterministic fuel price F , that is also used in our numerical experiments. Then the state of the control problem is reduced to $X = (R, P, Y')'$ with values in the state space $\mathcal{X} \subset \mathbb{R}^{\ell+2}$. A generalization to the full model including F as state is straightforward.

The idea is to divide the state space into a finite number of disjoint subsets, each represented by a single point, in which we want to compute approximations of the value function V and the optimal decision rule $\tilde{\alpha}$. This approach leads to an approximate MDP with a finite state space and a finite-state Markov chain as state process.

The construction of the state space partition is based on an $(\ell + 2)$ -dimensional grid. We choose for each of the $\ell + 2$ state variables $\dagger = R, P, Y^1, \dots, Y^\ell$ discretization parameters $N_\dagger \in \mathbb{N}$, sets of indices $\mathcal{N}_\dagger = \{0, \dots, N_\dagger\}$, and define the points $r_0 < \dots < r_{N_R} \in [r, \bar{r}]$, $p_0 < \dots < p_{N_P}$ in $[p, \bar{p}]$, $y_0^k < \dots < y_{N_{Y^k}}^k$ in \mathbb{R} , $k = 1, \dots, \ell$. Then, the $(\ell + 2)$ -dimensional discretized state space is given by the grid

$$\hat{\mathcal{X}} = \{r_0, \dots, r_{N_R}\} \times \{p_0, \dots, p_{N_P}\} \times \{y_0^1, \dots, y_{N_{Y^1}}^1\} \times \dots \times \{y_0^\ell, \dots, y_{N_{Y^\ell}}^\ell\}.$$

Each point $x_m = (r_i, p_j, y_{k_1}^1, \dots, y_{k_\ell}^\ell)' \in \hat{\mathcal{X}}$ is identified by the multi-index $m = (i, j, k_1, \dots, k_\ell) \in \hat{\mathcal{N}}$ where $\hat{\mathcal{N}} = \mathcal{N}_R \times \mathcal{N}_P \times \mathcal{N}_{Y^1} \times \dots \times \mathcal{N}_{Y^\ell}$ is the set of $(\ell + 2)$ -tuples of multi-indices.

For the construction of the discretized state process denoted by $\hat{X} = (\hat{R}, \hat{P}, \hat{Y}')'$ we map all values of the original state $X \in \mathcal{X}$ coordinate-wise to the next grid point. Then, each grid point x_m represents a rectangular neighborhood or box around x_m . For grid points at the boundary these neighborhoods collect all points of \mathcal{X} beyond the boundary. Figure 7.1 sketches the projection of the computational grid onto the (r, p) -plane \mathcal{X}_{RP} for fixed y^1, \dots, y^ℓ .

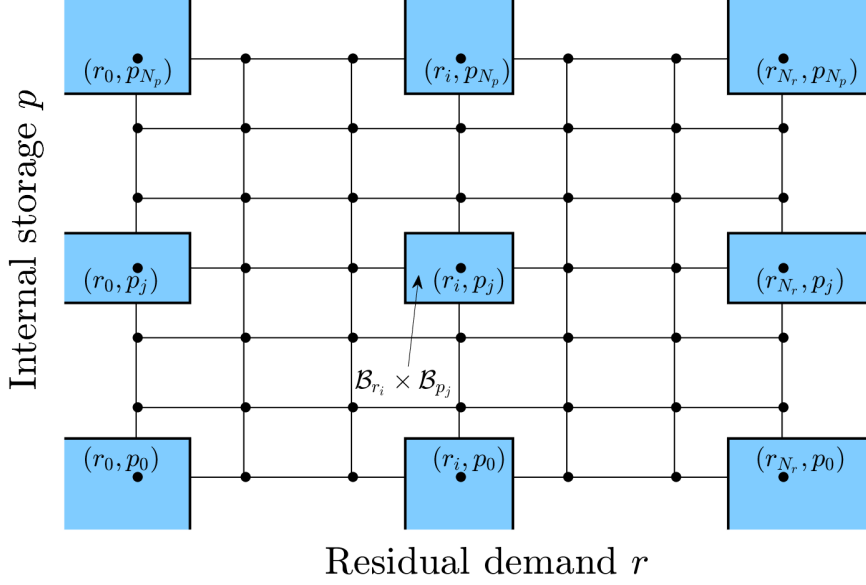


Figure 7.1. Projection of the computational grid onto (r, p) -plane \mathcal{X}_{RP} for fixed y^1, \dots, y^ℓ .

This approach can be formalized as follows. We distinguish inner grid points with indices in $\{1, \dots, N_\dagger - 1\}$, and boundary grid points including the corners for which at least one index is 1 or N_\dagger , $\dagger = R, P, Y^1, \dots, Y^\ell$. The neighborhoods of inner grid points r_i, p_j , and $y_{l^k}^k, k = 1, \dots, \ell$ are defined by $\mathcal{C}_i^R = (\frac{1}{2}(r_i + r_{i-1}), \frac{1}{2}(r_i + r_{i+1}))$, $\mathcal{C}_j^P = (\frac{1}{2}(p_j + p_{j-1}), \frac{1}{2}(p_j + p_{j+1}))$, $\mathcal{C}_{l^k}^{Y^k} = (\frac{1}{2}(y_{l^k}^k + y_{l^k-1}^k), \frac{1}{2}(y_{l^k}^k + y_{l^k+1}^k))$, for $i = 1, \dots, N_R - 1, j = 1, \dots, N_P - 1, l^k = 1, \dots, N_{Y^k} - 1, k = 1, \dots, \ell$. For the boundary grid points, we extend the domain to the respective boundaries of the original state space \mathcal{X} as follows

$$\begin{aligned} \mathcal{C}_0^R &= \left(-\infty, \frac{1}{2}(r_0 + r_1)\right], & \mathcal{C}_0^P &= \left(-\infty, \frac{1}{2}(p_0 + p_1)\right], & \mathcal{C}_0^{Y^k} &= \left(-\infty, \frac{1}{2}(y_0^k + y_1^k)\right], \\ \mathcal{C}_{N_R}^R &= \left(\frac{1}{2}(r_{N_R} + r_{N_R-1}), \infty\right), & \mathcal{C}_{N_P}^P &= \left(\frac{1}{2}(p_{N_P} + p_{N_P-1}), \infty\right), & \mathcal{C}_{N_{Y^k}}^{Y^k} &= \left(\frac{1}{2}(y_{N_{Y^k}}^k + y_{N_{Y^k}-1}^k), +\infty\right). \end{aligned}$$

The projection of the original state $X_n = (R_n, P_n, Y_n) \in \mathcal{X}$ onto the discretized state space $\widehat{\mathcal{X}}$ results in $\widehat{X}_n = (\widehat{R}_n, \widehat{P}_n, \widehat{Y}_n)'$ defined for $n = 0, \dots, N$ by

$$\widehat{R}_n = \sum_{i=0}^{N_R} r_i \mathbb{1}_{\mathcal{C}_i^R}(R_n), \quad \widehat{P}_n = \sum_{j=0}^{N_P} p_j \mathbb{1}_{\mathcal{C}_j^P}(P_n), \quad \widehat{Y}_n^k = \sum_{l=0}^{N_{Y^k}} y_l^k \mathbb{1}_{\mathcal{C}_l^{Y^k}}(Y_n^k), \quad k = 1, \dots, \ell. \quad (7.1)$$

This discretization converts the given MDP with state space \mathcal{X} into a MDP for a controlled finite-state Markov chain with state space $\widehat{\mathcal{X}}$. Combining the recursion (6.1) for the original state process with the projection formulas in (7.1), the dynamics of the discrete-state approximation (\widehat{X}_n) is given by the recursion

$$\widehat{X}_{n+1} = \widehat{\mathcal{T}}(n, \widehat{X}_n, \alpha_n, \mathcal{B}_{n+1}), \quad \widehat{X}_0 = \widehat{x}_0.$$

for $n = 0, \dots, N-1$. Here, $\widehat{\mathcal{T}} : \{0, \dots, N-1\} \times \widehat{\mathcal{X}} \times \mathcal{K} \times \mathbb{R}^3 \rightarrow \widehat{\mathcal{X}}$ is the discrete-state transition operator. It is for $n \in \{0, \dots, N-1\}$, $x = (r, p, y) \in \widehat{\mathcal{X}}$, $a \in \mathcal{K}$, $b \in \mathbb{R}^3$ defined as $\widehat{\mathcal{T}} = (\widehat{\mathcal{T}}^R, \widehat{\mathcal{T}}^P, (\widehat{\mathcal{T}}^Y)')$ with

$$\begin{aligned} \widehat{\mathcal{T}}^R(n, x, a, b) &= \sum_{i=0}^{N_R} r_i \mathbb{1}_{\mathcal{C}_i^R}(\mathcal{T}^R(n, x, a, b)), & \widehat{\mathcal{T}}^P(n, x, a, b) &= \sum_{j=0}^{N_P} p_j \mathbb{1}_{\mathcal{C}_j^P}(\mathcal{T}^P(n, x, a, b)), \\ \widehat{\mathcal{T}}^Y(n, x, a, b) &= \widetilde{\mathcal{T}}^Y(n, y, a) = \sum_{l=0}^{N_{Y^k}} y_l^k \mathbb{1}_{\mathcal{C}_l^{Y^k}}(\overline{\mathcal{T}}^Y(n, y, a)), & k &= 1, \dots, \ell, \end{aligned}$$

where $\mathcal{T}^R, \mathcal{T}^P, \overline{\mathcal{T}}^Y$ are given in (6.2), and \widehat{x}_0 is the projection of the initial state x_0 onto $\widehat{\mathcal{X}}$. Note that the discrete-state approximation (\widehat{X}_n) inherits the Markov property from the original state process (X_n) . This allows to characterize the transition kernel of the approximate MDP, that describes the conditional distribution of \widehat{X}_{n+1} given \widehat{X}_n and α_n , by the transition probabilities of the Markov chain. They are given for all multi-indices $m_1, m_2 \in \widehat{\mathcal{N}}$ by

$$\overline{P}_{m_1 m_2}^a = \mathbb{P}(\widehat{X}_{n+1}^\alpha = x_{m_2} \mid \widehat{X}_n^\alpha = x_{m_1}, \alpha_n = a) = \mathbb{P}(\widehat{\mathcal{T}}(n, x_{m_1}, a, \mathcal{B}_{n+1}) = x_{m_2}),$$

which are the probabilities that the state moves from x_{m_1} at time n to x_{m_2} at time $n+1$ under the action $\alpha_n = a$. For the computation of these probabilities one can utilize that the conditional distribution of the pair of projected state components $(\widehat{R}_{n+1}, \widehat{P}_{n+1})$, given the state \widehat{X}_n and the decision rule α_n at time n , follows from the bivariate Gaussian distribution of the original state variables (R_{n+1}, P_{n+1}) . Further, the corresponding conditional distribution of \widehat{Y}_{n+1} is degenerate, since Y and thus also its projection \widehat{Y} follows deterministic dynamics. To be more specific, suppose the two multi-indices are given for $\dagger = 1, 2$ as $m_\dagger = (i_\dagger, j_\dagger, l_\dagger^1, \dots, l_\dagger^\ell) \in \widehat{\mathcal{N}}$, and denote by $y_{m_\dagger} = (y_{l_\dagger^1}^1, \dots, y_{l_\dagger^\ell}^\ell)'$. Then it holds

$$\begin{aligned} \overline{P}_{m_1 m_2}^a &= \mathbb{P}(\widehat{\mathcal{T}}(n, x_{m_1}, a, \mathcal{B}_{n+1}) = x_{m_2} = (r_{i_2}, p_{j_2}, y_{l_2^1}^1, \dots, y_{l_2^\ell}^\ell)') \\ &= \mathbb{P}((\widehat{\mathcal{T}}^R(n, x_{m_1}, a, \mathcal{B}_{n+1}), \widehat{\mathcal{T}}^P(n, x_{m_1}, a, \mathcal{B}_{n+1}))' = (r_{i_2}, p_{j_2})) \mathbb{P}(\widetilde{\mathcal{T}}^Y(n, y_{m_1}, a) = y_{m_2}) \\ &= \mathbb{P}((\mathcal{T}^R(n, x_{m_1}, a, \mathcal{B}_{n+1}), \mathcal{T}^P(n, x_{m_1}, a, \mathcal{B}_{n+1})) \in \mathcal{C}_{r_{i_2}} \times \mathcal{C}_{p_{j_2}}) \mathbb{P}(\overline{\mathcal{T}}^Y(n, y_{m_1}, a) \in \prod_{k=1}^{\ell} \mathcal{C}_{l_2^k}^{Y^k}), \end{aligned}$$

For more details on the computation of the first probability in the last line, we refer to [28, Chapter 6]. For the last probability, the deterministic dynamics of Y and therefore of \widehat{Y} yields

$$\mathbb{P}(\overline{\mathcal{T}}^Y(n, y_{m_1}, a) \in \prod_{k=1}^{\ell} \mathcal{C}_{l_2^k}^{Y^k}) = \prod_{k=1}^{\ell} \mathbb{1}_{\mathcal{C}_{l_2^k}^{Y^k}}(\overline{\mathcal{T}}_k^Y(n, y_{m_1}, a)).$$

We are now able to construct approximations of the value function $V(n, x)$ and the optimal decision rule $\tilde{\alpha}(n, x)$ of the original MDP in the points of the discretized state space $\widehat{\mathcal{X}}$. These approximations are denoted accordingly by $\widehat{V}(n, x)$ and $\widehat{\alpha}(n, x)$. They are obtained by solving the Bellman equation for the approximate MDP. Analogous to the result given in Theorem 6.8, this leads to the following backward recursion for all grid points $x_m \in \widehat{\mathcal{X}}$ identified by an multi-index $m \in \widehat{\mathcal{N}}$.

$$\begin{aligned} \widehat{V}(N, x_m) &= \Phi_N(x_m), \\ \widehat{V}(n, x_m) &= \min_{a \in \mathcal{K}(n, x_m)} \left\{ \Psi(n, x, a) + \mathbb{E}[\widehat{V}(n+1, \widehat{\mathcal{T}}(n, x_m, a, \mathcal{B}_{n+1}))] \right\}, \quad n = N-1, \dots, 0. \end{aligned} \quad (7.2)$$

The optimal decision rule $\hat{\alpha}^*(n, x_m)$ is given by the minimizer in (7.2), and the expectation in (7.2) by $\mathbb{E}[\hat{V}(n+1, \hat{T}(n, x_m, a, \mathcal{B}_{n+1}))] = \sum_{x_q \in \hat{\mathcal{X}}} \bar{P}_{mq}^a \hat{V}(n+1, x_q)$.

8. Numerical Results

In this section, we present numerical results that illustrate the solution of the stochastic optimal control problem for the cost-optimal management of a residential heating system. In particular, we show approximations of the value function and the optimal decision rules obtained by solving the Bellman equation (7.2) for the approximate MDP that we studied in Section 7.

In order to keep the curse of dimensionality under control, we use for the approximation of the GES spatio-temporal temperature distribution Q by a reduced-order system of ODEs of dimension $\ell = 4$ and two output variables, representing the average temperature approximations in the storage medium Q^M and the average temperature in the PHX fluid Q^F . The latter serves as approximation of the average outlet temperature Q^O , which appears in the transition operator of the MDP. We consider a GES with one PHX, for which we have found that the 4-dimensional reduced-order system already provides quite good approximations for the two aggregated characteristics mentioned above. We also found that the naive approximation $Q^F \approx Q^O$ can be significantly improved using the following formula to reconstruct Q^O from Q^F

$$Q^O(t) \approx f(Q^F(t), a) \quad \text{with} \quad f(q, a) = \begin{cases} 2q - Q_C^I & a = -1, \\ q + \Delta_{HP}/2, & a = +1, \\ q & \text{otherwise.} \end{cases}$$

It results from the assumption of a perfect linear increase or decrease of the liquid temperature along the way through the PHX from the inlet to the outlet leading to the relation $Q^F = (Q^I + Q^O)/2$ with the inlet temperatures $Q^I = Q_C^I$ and $Q^O - \Delta_{HP}$ for $a = -1, +1$, and $Q^I = Q^O$ otherwise. Note that including the outlet temperature Q^O directly in the system output requires considerably larger dimensions ℓ of the reduced-order system, which then prevents a computationally tractable solution to the optimization problem.

Our numerical experiments are based on a model with a constant and known fuel price $F(t) = f_0 > 0$. This is the typical case for small and medium sized heating systems operating with fixed tariffs for fuel purchase. This makes it possible to remove the fuel price F from the state variables and reduce the state dimension by one, which in turn again helps to keep the curse of dimensionality under control. We work with a planning horizon of $T = 3$ days, which is divided into $N = 72$ periods of length $\Delta_N = 1$ hour. Since we consider a short-term simulation with a small horizon time, we neglect discounting as well as the seasonality effect of the residual demand and suppose $\mu_R(t) = \mu_0^R = \text{const}$.

For the computation of approximations of the value function and the optimal decision rule, we use the backward recursion following from Bellman equation (7.2) for the approximate MDP. The state space is discretized with $N_R = 8$, $N_P = 11$, $N_{Y1} = N_{Y2} = N_{Y3} = 4$, $N_{Y4} = 8$. The finer discretization of the range of Y^4 is motivated by the fact, that we use for the four-dimensional state space Y a coordinate system which is such that $C^M Y = c Y^4$ for some constant $c \in \mathbb{R}$. Thus, Y^4 is proportional to the average temperature in the storage medium $Q^M C^M Y$. Recall, the latter plays a crucial role in the construction of the set of feasible controls $\mathcal{K}^Y(n, x)$, see (6.8). The GES storage medium is selected as dry soil,

Parameters	Values	Units	Parameters	Values	Units
l_x, l_y, l_z	10, 1, 10	m	T	72	h
h_x, h_y	0.1, 0.01	m	N	72	
h_p	0.02	m	Δ_N	1	h
n_p	1		P_{in}, P_{out}	40, 30	$^{\circ}C$
ρ^M	2000	kg/m^3	ρ^F	998	kg/m^3
c_p^M	800	$J/(kgK)$	$c_p^F = c_p^W$	4182	$J/(kgK)$
κ^M	1.59	$J/(smK)$	κ^F	0.60	$J/(mK)$
d^M	9.9375×10^{-7}	m^2/s	d^F	1.4376×10^{-7}	m^2/s
\bar{v}_0	10^{-2}	m/s	Q_C^I	40	$^{\circ}C$
λ^G	10	$J/(sm^2 K)$	Δ_{HP}	3	K
Q_0	10	$^{\circ}C$	Q^G	15	$^{\circ}C$
σ_R	232.5	$J/\sqrt{s^3}$	μ_R^0	-4.64×10^3	J/s
β_R	0.5	$1/h$	A^P	9.096	m^2
m^P	4000	kg	κ^P	12	$J/(sm^2 K)$
m^Q	200000	kg	ξ_F	30	l/h
p_{ref}	60	$^{\circ}C$	ξ_{HP}	3	EUR/K
q_{ref}	20	$^{\circ}C$	ξ_P	5	EUR/h
P_{amb}	20	$^{\circ}C$	ξ_{pen}^P, ξ_{pen}^Q	6.7, 0.45	EUR/kWh
f_0	2.25	EUR/l	$\xi_{liq}^P = \xi_{liq}^Q$	0	EUR/kWh
ε	0.05		\bar{p}	90	$^{\circ}C$
γ	3.27×10^{-6}	$1/s$	\underline{p}	30	$^{\circ}C$
L_C	1.66×10^3	$J/(Ks)$	\underline{q}	10	$^{\circ}C$
L_F	7.436×10^4	J/s	\bar{q}	30	$^{\circ}C$
L_D	1.39×10^3	$J/(Ks)$	\underline{r}	-16.7	MJ
δ	0		\bar{r}	13.4	MJ

Table 8.1. Model and discretization parameters

the PHX fluid is water, the PHX height is $h_p = 0.02 m$. The GES is a cuboid with edge lengths $l_x = 10 m, l_y = 1 m, l_z = 10 m$, the spatial discretization of the heat equation on the two-dimensional cross-section uses step sizes $h_x = 0.1 m, h_y = 0.01 m$. The heat pump spread is set to $3K$, as it is often observed in reality. A penalty is chosen for the final cost. It is incurred if the IES and GES are not filled properly. No liquidation revenues are realized for leftover energy. The other model parameters are given in Table 8.1.

In the following we present results for full and empty storage, characterized by $Q_N^M = \bar{q} = 30^{\circ}C$ and $Q_N^M = \underline{q} = 10^{\circ}C$, respectively. Furthermore, results are shown for an intermediate grid point for the reduced order state y which corresponds to the average temperature $C^M y = 18^{\circ}C$ of the GES medium, and is close to the midpoint $(\underline{q} + \bar{q})/2$ and therefore referred to as ‘‘half full GES’’.

Terminal cost function. The left panel of Fig. 8.1 shows the terminal cost function $\phi_N(x)$ as a function of (\tilde{r}, p) . for an empty, half full and full GES. Here, $\tilde{r} = \mu_R^0 + r$ denotes the residual demand including the seasonality component. The right panel of shows the dependence of the terminal costs on the storage level in IES and GES at terminal time, that is on $P_N = p$ and $Q_N^M = \bar{q}^M = C^M y$. This figure shows that the terminal cost function is zero when the average IES and GES temperature are both above the threshold ($P_N \geq p_{ref} = 60^{\circ}C$ and $Q_N^M \geq q_{ref} = 20^{\circ}C$). However, it begins to increase linearly when these temperatures fall below their respective threshold values.

Value function and optimal decision rule at time $n = N - 1$. Fig. 8.2 shows results at the beginning of the last period starting at time $T - \Delta t = 71h$. The top left panel depicts the approximations of the value function $V(n, x)$ as a function of (\tilde{r}, p) for a full GES, a half full GES, and an empty GES. The other panels show the approximate optimal decision rules $\tilde{\alpha}(n, x)$ as functions of (\tilde{r}, p) , for a full GES,

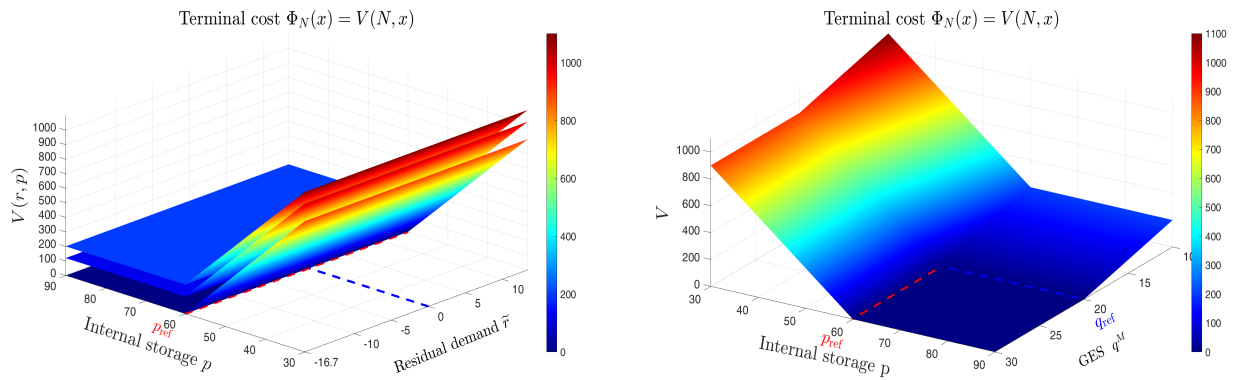


Figure 8.1. Terminal cost function $\Phi_N(x) = V(N, x)$.

Left: depending on (\tilde{r}, p) for empty, half full and full GES (upper, middle, lower graph).
 Right: depending on p and average GES temperature $C^M y$.

a half full GES, and an empty GES in separate panels.

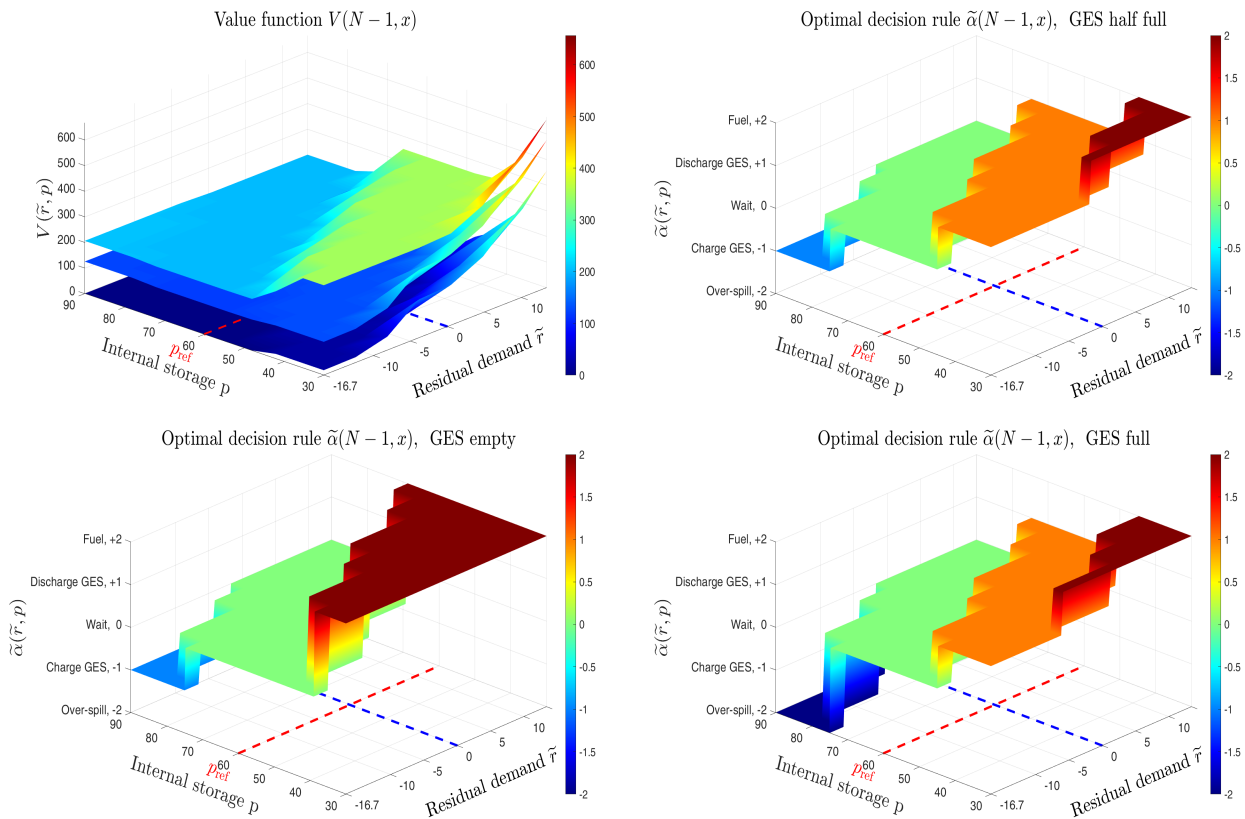


Figure 8.2. Value function $V(n, x)$ and optimal decision rule $\tilde{\alpha}^*(n, x)$ at time $n = N - 1$ as a function of (\tilde{r}, p) for different GES filling levels.

Top left: Value function for empty, half full and full GES (upper, middle, lower graph).

Bottom left, top right, bottom right: Optimal decision rules for empty, half full and full GES.

For $n = N - 1$ the Bellman equation (7.2) yields for the value function $\hat{V}(N - 1, x) = \Psi(n, x, a^*) +$

$\mathbb{E}[\Phi_N(\widehat{\mathcal{T}}(N-1, x, a^*, \mathcal{B}_{N+1}))]$ where a^* denotes the optimal action. This decomposition into the running costs in the last period and the expected terminal costs helps to explain the properties of the value function. It can be observed that the value function is almost constant when the IES temperature exceeds the penalty threshold $p_{\text{ref}} = 60^\circ\text{C}$, and the residual demand is negative (overproduction). In that case, it is optimal to wait ($a = 0$), to transfer thermal energy to the GES ($a = -1$), or even to apply over-spilling when the IES is almost full and there is a large negative residual demand, which indicates a strong overproduction of heat. For these controls no, or only very small further running costs are incurred in the last period. Therefore, the value function represents the expected terminal penalties to be paid if the average GES temperature is below q_{ref} . The latter does not depend on (\tilde{r}, p) , but only on the reduced-order state y which explains the different constant levels of the the value function.

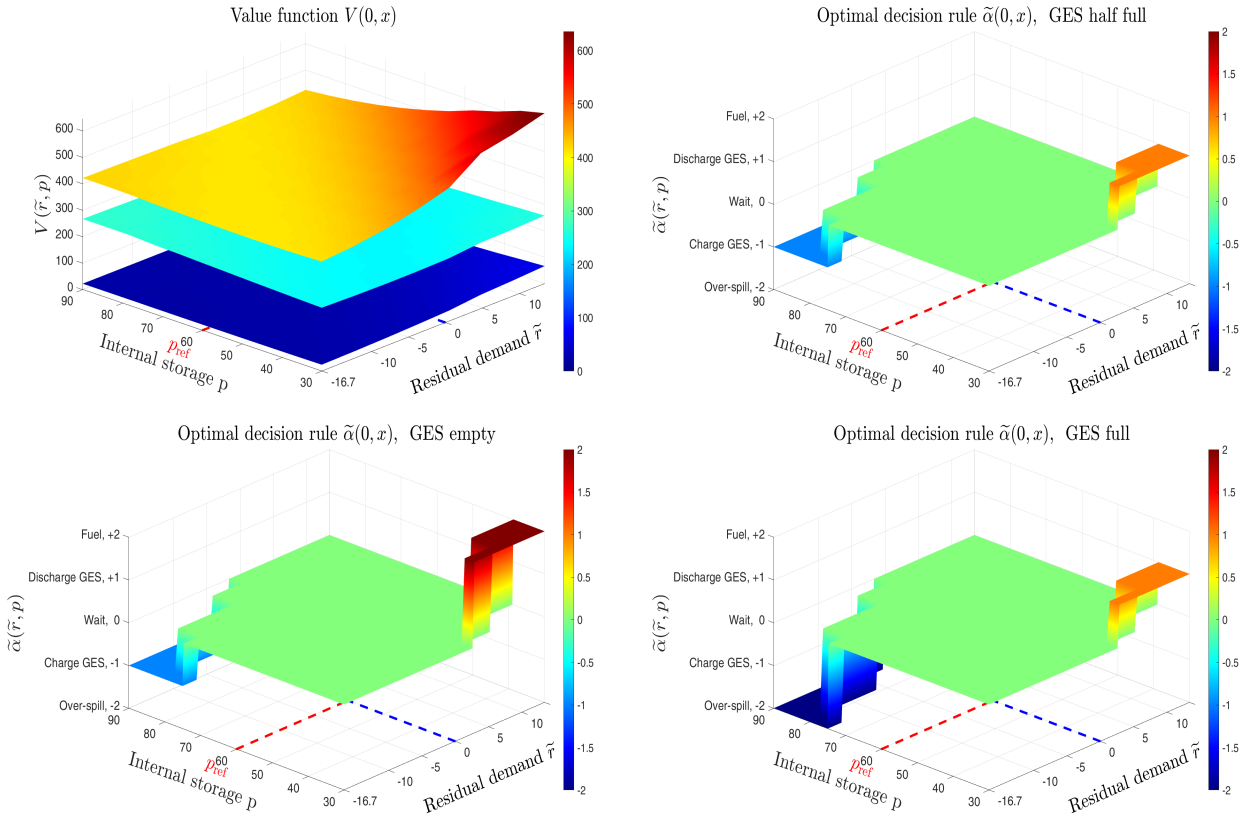


Figure 8.3. Value function $V(n, x)$ and optimal decision rule $\tilde{\alpha}^*(n, x)$ at initial time $n = 0$ as a function of (\tilde{r}, p) for different GES filling levels.

Top left: Value function for empty, half full and full GES (upper, middle, lower graph).

Bottom left, top right, bottom right: Optimal decision rules for empty, half full and full GES.

When the residual demand becomes positive and when the IES temperature falls below p_{ref} then it is optimal to charge the IES in order to avoid penalty payments at the end of the period if the IES temperature remains below p_{ref} . Considering the chosen parameters for the operating costs, burning fuel ($a = +2$) to charge the IES is more expensive than transferring heat from the GES to the IES with the heat pump ($a = +1$). Therefore, as expected, it is optimal to use the heat pump to charge the IES when its temperature is moderately low, especially when the residual demand is positive, which means

that the heat supply does not cover the demand. Only when the IES is almost completely empty or the residual demand is very high, it is optimal to choose the expensive option of fuel firing. This also explains that the value function increases with decreasing IES temperature p and increasing residual demand \tilde{r} . The strong growth of the value function with strong unsatisfied demand and almost empty IES results from the penalties that must be paid if the IES temperature cannot be raised to p_{ref} within the last period. Note that when the GES is empty then firing fuel is the only available option to charge the IES, as can be seen in the top right-hand panel.

Value function and optimal decision rule at initial time $\mathbf{n} = \mathbf{0}$. Fig. 8.3 shows the approximate value function and optimal decision rules as functions of (\tilde{r}, p) at the initial time $t = 0$ h for a full GES, a half full GES, and an empty GES. In contrast to the results for $n = N - 1$, the value functions shown in the top left-hand box now take on larger values for IES temperatures above p_{ref} , as there are 72 periods ahead in which there is a potential imbalance between supply and demand and therefore ongoing costs could be incurred. On the other hand, the maximum values which are attained for very small IES temperatures are smaller now, since penalties at terminal time can be avoided by an active storage management. The increase with decreasing IES temperature p is much less pronounced and visible only for positive residual demand. In contrast, the value function increases visibly with increasing residual demand \tilde{r} , especially for very high unsatisfied demand and low IES temperatures. This is due to the fact that in this case the transfer of heat from the GES to the IES with the help of the heat pump or even by firing fuel in the next, or one of the next periods, is optimal and causes corresponding running costs. The optimal decision rules show that it is only not optimal to wait when the IES is almost full or almost empty. In these cases, heat exchange with the GES is optimal unless the GES is full or empty. With a full GES, the only feasible and therefore optimal action is over-spilling, while with an empty GES, firing fuel is the only option.

Optimal Paths of the State Process. Fig. 8.4 shows optimal paths of the average temperatures in the IES and GES together with the residual demand when we start with almost empty IES and GES. Then in the first periods it is optimal to wait when there is overproduction ($\tilde{R} < 0$) and to fire fuel when there is unsatisfied demand ($\tilde{R} > 0$). After the initial phase, with an almost empty IES and for small positive residual demand, it is optimal to discharge the GES and do not fire fuel until it is not almost empty. When the IES is almost full and the residual demand is negative, it is optimal to transfer heat from the IES to the GES.

9. Summary and Outlook

We have investigated a stochastic optimal control problem for the cost-optimal management of a residential heating system under stochastic supply-demand imbalance and stochastic energy prices. As a special feature, the heating system is equipped with a geothermal storage with a large capacity, whose response to charging and discharging decisions, however, depends on the spatial temperature distribution in the storage. The dynamics of the latter is described by a heat equation with a convection term that models the fluid movement in the PHX. This leads to a challenging, non-standard mathematical optimization problem. We first performed a semi-discretization of the heat equation and used model reduction techniques to reduce the dimension of the associated high-dimensional system of ODEs. Finally, a time discretization leads to a MDP, which was finally approximated by an MDP with a discretized state space. In this way, the curse of dimensionality is overcome and the optimal

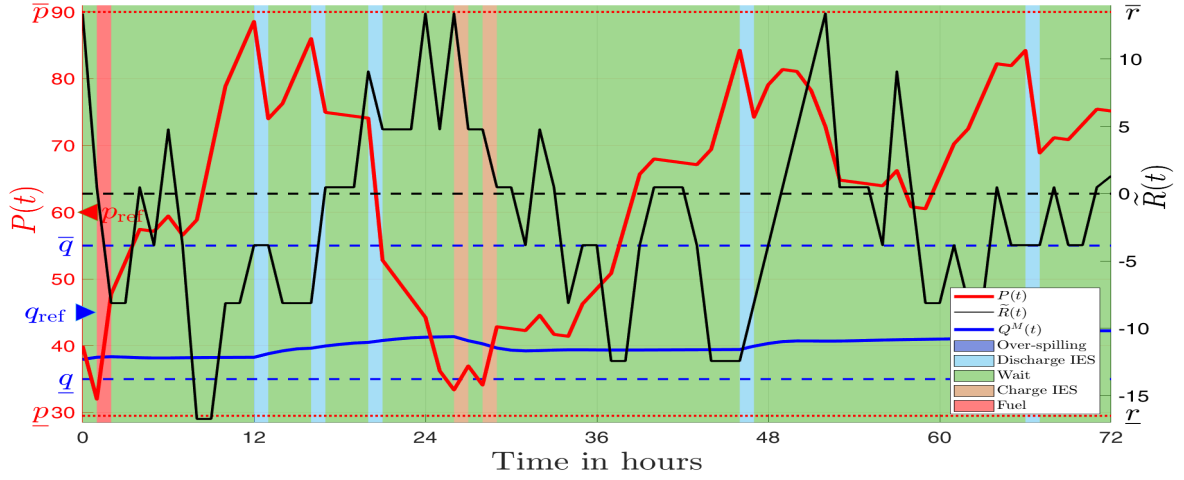


Figure 8.4. Optimal paths of IES temperature P (red), GES average temperature Q^M (blue) for initially almost empty IES ($P_0 = 40$ °C) and GES ($Q_0^M = 12$ °C). Red dashed lines at $\underline{p} = 30$ °C and $\bar{p} = 90$ °C represent state constraints for P , as well as the truncation values for the residual demand \tilde{R} at $\mu_R^0 + \underline{r} = -16.7$ and $\mu_R^0 + \bar{r} = 13.4$. The path of \tilde{R} (black) starts at $\tilde{R}(0) = \bar{r}$. The zero level of \tilde{R} is shown by a black dashed line. Blue dashed lines depict the state constraint $Q^M \in [q, \bar{q}]$. The background colors represent the optimal controls as shown in the legend.

control problem is solved numerically with a reasonable computational effort.

We are currently working on more realistic mathematical models of the geothermal storage taking into account the three-dimensional spatial temperature distribution in the storage and a refined topology of the PHXs. However, this will then lead to considerably higher dimensions of the state space of the control problem, and require more efficient approximation techniques to solve the control problem, such as optimal quantization, see Pages et al. [19] and reinforcement learning methods such as Q-learning, see Powell [22] and Sutton and Barto [27]. For some first results in this direction, we refer to Pilling et al. [21].

Acknowledgments The authors thank Martin Redmann (Martin-Luther University Halle–Wittenberg), Olivier Menoukeu Pamen (University of Liverpool), Gerd Wachsmuth, Eric Pilling and Andreas Künnemann (BTU Cottbus–Senftenberg) for valuable discussions that improved this paper.

Funding P.H. Takam gratefully acknowledges the support by the German Academic Exchange Service (DAAD), award number 57417894. R. Wunderlich gratefully acknowledges the support by the Federal Ministry of Education and Research (BMBF), award number 05M2022.

References

1. BÄHR, M., AND BREUSS, M. Efficient long-term simulation of the heat equation with application in geothermal energy storage. *Mathematics* 10, 13 (2022), 2309.

2. BÄHR, M., BREUSS, M., AND WUNDERLICH, R. Fast explicit diffusion for long-time integration of parabolic problems. In *International Conference of Numerical Analysis and Applied Mathematics (ICNAAM 2016)* (2017), vol. 1863, p. 410002.
3. BÄUERLE, N., AND RIEDER, U. *Markov Decision Processes With Applications to Finance*. Springer Science & Business Media, 2011.
4. BÄUERLE, N., AND RIESS, V. Gas storage valuation with regime switching. *Energy Systems* 7, 3 (2016), 499–528.
5. BAZRI, S., BADRUDDIN, I. A., USMANI, A. Y., KHAN, S. A., KAMANGAR, S., NAGHAVI, M. S., MALLAH, A. R., AND ABDELRAZEK, A. H. Thermal hysteresis analysis of finned-heat-pipe-assisted latent heat thermal energy storage application for solar water heater system. *Case Studies in Thermal Engineering* 40 (2022), 102490.
6. CHEN, Z., AND FORSYTH, P. A. A semi-Lagrangian approach for natural gas storage valuation and optimal operation. *SIAM Journal on Scientific Computing* 30, 1 (2007), 339–368.
7. CHEN, Z., AND FORSYTH, P. A. Implications of a regime-switching model on natural gas storage valuation and optimal operation. *Quantitative Finance* 10, 2 (2010), 159–176.
8. DINCER, I., AND ROSEN, M. A. *Thermal Energy Storage: Systems and Applications*. John Wiley & Sons, 2021.
9. EHSAN, A., AND YANG, Q. Scenario-based investment planning of isolated multi-energy microgrids considering electricity, heating and cooling demand. *Applied energy* 235 (2019), 1277–1288.
10. FLEMING, W. H., AND SONER, H. M. *Controlled Markov Processes and Viscosity Solutions*, vol. 25. Springer Science and Business Media, 2006.
11. GANET SOMÉ, M. Stochastic optimal control of prosumers in a district heating system. *arXiv.2501.09088* (2025).
12. GU, W., WU, Z., BO, R., LIU, W., ZHOU, G., CHEN, W., AND WU, Z. Modeling, planning and optimal energy management of combined cooling, heating and power microgrid: A review. *International Journal of Electrical Power & Energy Systems* 54 (2014), 26–37.
13. GUELPA, E., AND VERDA, V. Thermal energy storage in district heating and cooling systems: A review. *Applied Energy* 252 (2019), 113474.
14. HERNÁNDEZ-LERMA, O., AND LASSERRE, J. B. *Discrete-Time Markov Control Processes*. Springer New York, 1996.
15. KITAPBAYEV, Y., MORIARTY, J., AND MANCARELLA, P. Stochastic control and real options valuation of thermal storage-enabled demand response from flexible district energy systems. *Applied Energy* 137 (2015), 823 – 831.
16. KUANG, J., ZHANG, C., AND SUN, B. Stochastic dynamic solution for off-design operation optimization of combined cooling, heating, and power systems with energy storage. *Applied Thermal Engineering* 163 (2019), 114356.
17. MAJOR, M., POULSEN, S. E., AND BALLING, N. A numerical investigation of combined heat storage and extraction in deep geothermal reservoirs. *Geothermal Energy* 6, 1 (2018), 1–16.
18. OKSENDAL, B., AND SULEM, A. *Applied Stochastic Control of Jump Diffusions*. Springer International Publishing, 2019.

-
19. PAGES, G., PHAM, H., AND PRINTEMS, J. An optimal Markovian quantization algorithm for multi-dimensional stochastic control problems. *Stochastics and dynamics* 4, 04 (2004), 501–545.
 20. PHAM, H. *Continuous-Time Stochastic Control and Optimization With Financial Applications*, vol. 61. Springer Science and Business Media, 2009.
 21. PILLING, E., BÄHR, M., AND WUNDERLICH, R. Stochastic optimal control of an industrial power-to-heat system with high-temperature heat pump and thermal energy storage. *arXiv.2411.02211* (2024).
 22. POWELL, W. B. *Approximate Dynamic Programming: Solving the Curses of Dimensionality*. Wiley, Aug. 2011.
 23. PUTERMAN, M. L. *Markov Decision Processes: Discrete Stochastic Dynamic Programming*. John Wiley & Sons, 2014.
 24. REGNIER, G., SALINAS, P., JACQUEMYN, C., AND JACKSON, M. Numerical simulation of aquifer thermal energy storage using surface-based geologic modelling and dynamic mesh optimisation. *Hydrogeology Journal* 30, 4 (2022), 1179–1198.
 25. SHARDIN, A. A., AND WUNDERLICH, R. Partially observable stochastic optimal control problems for an energy storage. *Stochastics* 89, 1 (2017), 280–310.
 26. SOLTANI, M., MORADI KASHKOOLI, F., DEGHANI-SANIJ, A., NOKHOSTEEN, A., AHMADI-JOUGHJI, A., GHARALI, K., MAHBAZ, S., AND DUSSEAULT, M. A comprehensive review of geothermal energy evolution and development. *International Journal of Green Energy* 16, 13 (2019), 971–1009.
 27. SUTTON, R. S., AND BARTO, A. G. *Reinforcement Learning: An Introduction*. MIT press, 2018.
 28. TAKAM, P. H. *Stochastic optimal control problems of residential heating systems with a geothermal energy storage*. PhD thesis, BTU Cottbus-Senftenberg, 2023. <https://doi.org/10.26127/BTUopen-6450>.
 29. TAKAM, P. H., AND WUNDERLICH, R. Model order reduction for the input–output behavior of a geothermal energy storage. *Journal of Engineering Mathematics* (2024).
 30. TAKAM, P. H., AND WUNDERLICH, R. Numerical simulation of the input-output behavior of a geothermal energy storage. *Under revision* (2025).
 31. TAKAM, P. H., WUNDERLICH, R., AND PAMEN, O. M. Modeling and simulation of the input-output behavior of a geothermal energy storage. *Mathematical Methods in the Applied Sciences* (2023).
 32. TESTI, D., URBANUCCI, L., GIOLA, C., SCHITO, E., AND CONTI, P. Stochastic optimal integration of decentralized heat pumps in a smart thermal and electric micro-grid. *Energy Conversion and Management* 210 (2020), 112734.
 33. WARE, A. Accurate semi-Lagrangian time stepping for stochastic optimal control problems with application to the valuation of natural gas storage. *SIAM Journal on Financial Mathematics* 4, 1 (2013), 427–451.
 34. ZAYED, M. E., SHBOUL, B., YIN, H., ZHAO, J., AND ZAYED, A. A. Recent advances in geothermal energy reservoirs modeling: Challenges and potential of thermo-fluid integrated models

for reservoir heat extraction and geothermal energy piles design. *Journal of Energy Storage* 62 (2023), 106835.

35. ZHONG, J., TAN, Y., LI, Y., CAO, Y., PENG, Y., ZENG, Z., NAKANISHI, Y., AND ZHOU, Y. Distributed operation for integrated electricity and heat system with hybrid stochastic/robust optimization. *International Journal of Electrical Power & Energy Systems* 128 (2021), 106680.

A. List of Notations

t, T	time, horizon time
R, \tilde{R}	residual demand: deseasonalized/including seasonality
F, \tilde{F}	fuel price: deseasonalized/including seasonality
P	average temperature in the IES
$Q = Q(t, x, y)$	temperature in the GES
l_x, l_y, l_z	width, height and depth of the storage
h_P	PHX height
$\mathcal{D} = (0, l_x) \times (0, l_y)$	two-dimensional GES domain
$\mathcal{D}^M, \mathcal{D}^F, \mathcal{D}^J$	domain of storage medium, PHX fluid, interface in between
$\partial \mathcal{D}$	boundary of GES domain
$\partial \mathcal{D}^I, \partial \mathcal{D}^O$	inlet and outlet boundaries of PHX
$\partial \mathcal{D}^L, \partial \mathcal{D}^R, \partial \mathcal{D}^T, \partial \mathcal{D}^B$	left, right, top and bottom boundaries of the domain
$v = v_0(t)(v^x, v^y)'$	time-dependent velocity vector
\bar{v}_0	constant velocity during pumping
c_p^M, c_p^F, c_p^W	specific heat capacity of the storage fluid, PHX fluid, IES fluid
ρ^F, ρ^M	mass density of the fluid and medium
κ^F, κ^M	thermal conductivity of the fluid and medium
d^F, d^M	thermal diffusivity of the fluid and medium
λ^G	heat transfer coefficient between storage and underground
Q_0, Q^G	initial and underground temperature distribution of the GES
Q_C^I	inlet temperature of the PHX during charging
$\bar{Q}^M, \bar{Q}^F, \bar{Q}^O$	average temperature in GES storage medium, PHX fluid, GES outlet
Q^M, Q^F, Q^O	respective approximations from reduced-order system
Δ_{HP}	heat pump spread
P_{in}, P_{out}, P_{amb}	IES inflow, outflow and ambient temperature
γ	rate of IES heat loss to the environment
η_{\dagger}	drift coefficient $\dagger = P, Y$
A, B, C	$n \times n$ system matrix, $n \times m$ input matrix, $n_O \times n$ output matrix
Y, Z	state and output of reduced-order system
ℓ, n_O	dimension of state Y and output Z
g	input variable of the system
\mathbb{P}, \mathbb{E}	probability measure, expectation
W_R, W_F	Wiener processes
$\mu_{R/F}, \beta_{R/F}, \sigma_{R/F}$	mean reversion level, speed and volatility for residual demand/ fuel
N, Δ_N	number of time intervals, time step size
$\mathcal{X}, \hat{\mathcal{X}}$	state space of continuous and discretized state
$X = X(t) = (R, F, P, Y)'$	continuous-time state process at time t
$X_n = (R_n, F_n, P_n, Y_n)'$	discrete-time state process at time t_n
$\hat{X}_n = (\hat{R}_n, \hat{F}_n, \hat{P}_n, \hat{Y}_n)'$	discrete-time state process on discretized state space
$\mathcal{B} = (\mathcal{B}_n)_{n=1, \dots, N}$	sequence of independent Gaussian random vectors
$m_{\dagger}(n), \Sigma_{\dagger}^2(n)$	conditional mean and variance of the random variables \dagger_{n+1} , with $\dagger = R, F$
$\Sigma_P^2(n, a), \rho(n, a)$	conditional covariance, correlation coefficient of R_{n+1} and P_{n+1}
$\mathcal{T} = (\mathcal{T}^R, \mathcal{T}^F, \mathcal{T}^P, (\mathcal{T}^Y)')$	transition operator
$u = (u(t))_{t \in [0, T]}$	continuous-time control process

$\mathcal{K}(n, x), \mathcal{K}_P(n, x), \mathcal{K}_Y(n, x)$	state-dependent set of feasible actions
$\alpha = (\alpha_1, \dots, \alpha_{N-1}), \tilde{\alpha}(n, x)$	discrete-time control process, decision rule
\mathcal{A}	set of admissible controls
ξ_{\dagger}	price, price rates
$\psi, \Psi, \phi_N, \Phi_N$	continuous-time/ discrete-time running and terminal cost
$J(n, x; u), V(n, x)$	performance criterion and value function at time n
$\mathcal{N}_{\dagger} = \{0, 1, \dots, N_{\dagger}\}$	set of indices for states $\dagger = R, P, Y^1, \dots, Y^{\ell}$
$\mathcal{N}_R \times \mathcal{N}_P \times \mathcal{N}_{Y^1} \times \dots \times \mathcal{N}_{Y^{\ell}}$	set of multi-indices for points of discretized space \widehat{X}
$x_m = (r_i, p_j, y_{k_1}^1, \dots, y_{k_{\ell}}^{\ell})$	point of discretized space \widehat{X}
\bar{P}_{m_1, m_2}^a	transition probability
\mathcal{C}_{\dagger_i}	neighborhood of $\dagger_i, i = 0, \dots, N_{\dagger}$ with $\dagger = r, p, y^k$
\mathbb{I}_n	n -dimensional identity matrix

Abbreviations

PHX	Pipe heat exchanger
MDP	Markov decision process
IES, GES	Internal, Geothermal storage
ODE, PDE, SDE	Ordinary, partial, stochastic differential equation

B. Details on the Transition Operator

The functions $\Sigma_R(n), \Sigma_F(n), \Sigma_P(n, a), \rho(n, a)$ and \mathcal{H} appearing in the transition operator in (6.2) of Proposition 6.3 are given by

$$\begin{aligned}\Sigma_{\dagger}^2(n) &= \frac{\sigma_{\dagger, n}^2}{2\beta_{\dagger}}(1 - e^{-2\beta_{\dagger}\Delta_N}), \quad \dagger = R, F, \\ \Sigma_P^2(n, a) &= \frac{\zeta_P^2 \sigma_{R, n}^2}{2\beta_R(\beta_R - \gamma)^2(\beta_R + \gamma)} \left\{ \gamma + 4\beta_R e^{-(\beta_R + \gamma)\Delta_N} - (\beta_R + \gamma)e^{-2\beta_R\Delta_N} \right. \\ &\quad \left. - \beta_R(2 + e^{-2\gamma\Delta_N}) + \frac{\beta_R^2}{\gamma}(1 - e^{-2\gamma\Delta_N}) \right\}, \\ \Sigma_{RP}^2(n, a) &= -\frac{\zeta_P \sigma_{R, n}^2}{2\beta_R(\beta_R^2 - \gamma^2)} \left(\beta_R - \gamma - 2\beta_R e^{-(\beta_R + \gamma)\Delta_N} + (\beta_R + \gamma)e^{-2\beta_R\Delta_N} \right), \\ \rho(n, a) &= \frac{\Sigma_{RP}^2(n, a)}{\Sigma_R(n)\Sigma_P(n, a)}.\end{aligned}$$

The function $\mathcal{H} : \{0, \dots, N-1\} \times \mathbb{R}^{\ell+1} \times \mathcal{K} \rightarrow \mathbb{R}$ is linear in the state components r, y and given by

$$\mathcal{H}(n, r, y, a) = \begin{cases} h(n, r) + (P_{\text{amb}} + \frac{\zeta_F}{\gamma})(1 - e^{-\gamma\Delta_N}), & a = +2 \\ h(n, r) + (P_{\text{amb}} + \frac{\zeta_C(p_{\text{in}} - P_{\text{out}})}{\gamma})(1 - e^{-\gamma\Delta_N}), & a = +1 \\ h(n, r) + P_{\text{amb}}(1 - e^{-\gamma\Delta_N}), & a = 0 \\ h(n, r) + (P_{\text{amb}} - \frac{\zeta_D Q_C}{\gamma})(1 - e^{-\gamma\Delta_N}) + e^{-\gamma\Delta_N} \psi(n, y), & a = -1, \\ e^{-\gamma\Delta_N}(p + P_{\text{amb}}(e^{\gamma\Delta_N} - 1)) & a = -2, \end{cases}$$

$$\text{with } h(n, r) = \frac{\zeta_{PF}}{\beta_R - \gamma} (e^{-\beta_R\Delta_N} - e^{-\gamma\Delta_N}) - \frac{\zeta_{PF}\mu_{R, n}}{\gamma} (1 - e^{-\gamma\Delta_N})$$

$$\text{and } \psi(n, y) = \zeta_D C^O \left\{ (e^{(\mathbb{Y}_{\ell} + \bar{A})\Delta_N} - \mathbb{I}_{\ell})(\gamma \mathbb{I}_{\ell} + \bar{A})^{-1} y + \right. \\ \left. [(e^{(\gamma \mathbb{I}_{\ell} + \bar{A})\Delta_N} - \mathbb{I}_{\ell})(\gamma \mathbb{I}_{\ell} + \bar{A})^{-1} - \frac{1}{\gamma}(e^{\gamma\Delta_N} - 1)\mathbb{I}_{\ell}] \bar{A}^{-1} B g(n, -1) \right\}.$$

C. Proof of Lemma 6.6

Proof. Let $k = 0, \dots, N-1, x = (r, f, p, y)' \in \mathcal{X}, a \in \mathcal{K}$. Then

$$\bar{\Psi}(k, x, a) = e^{\delta k \Delta_N} \Psi(k, x, a) = e^{\delta t_k} \mathbb{E}_{k,x} \left[\int_{t_k}^{t_{k+1}} e^{-\delta s} \psi(X^{\bar{u}}(s), a) ds \right] = \int_{t_k}^{t_{k+1}} e^{-\delta(s-t_k)} \mathbb{E}_{k,x} \left[\psi(X^{\bar{u}}(s), a) \right] ds.$$

For $a = +2$, $\mu_{F,k} = \mu_F(t_k)$, $\Delta_N = t_{k+1} - t_k$, and using the fact that $M_t^F = \int_{t_k}^t e^{-\beta_F(s-\tau)} dW_F(\tau)$ is a martingale, we have

$$\begin{aligned} \bar{\Psi}(k, x, a) &= \int_{t_k}^{t_{k+1}} e^{-\delta(s-t_k)} \mathbb{E}_{k,x} [\psi(X^{\bar{u}}(s), a)] ds = \xi_F \int_{t_k}^{t_{k+1}} e^{-\delta(s-t_k)} \mathbb{E}[\mu_F(s) + F(s) \mid F(t_k) = f] ds \\ &= \xi_F \int_{t_k}^{t_{k+1}} e^{-\delta(s-t_k)} \mathbb{E} \left[\mu_F(s) + f e^{-\beta_F(s-t_k)} + \int_{t_k}^s \sigma_F(\tau) e^{-\beta_F(s-\tau)} dW_F(\tau) \right] ds \\ &= \xi_F \int_{t_k}^{t_{k+1}} e^{-\delta(s-t_k)} \left(\mu_F(s) + f e^{-\beta_F(s-t_k)} \right) ds = \xi_F \left[\frac{\mu_{F,k}}{\delta} (1 - e^{-\delta \Delta_N}) + \frac{f}{\delta + \beta_F} (1 - e^{-(\delta + \beta_F) \Delta_N}) \right] \end{aligned}$$

For $a = +1$, we have

$$\begin{aligned} \bar{\Psi}(k, x, a) &= \int_{t_k}^{t_{k+1}} e^{-\delta(s-t_k)} \mathbb{E}_{k,x} [\psi(X^{\bar{u}}(s), a)] ds = \int_{t_k}^{t_{k+1}} e^{-\delta(s-t_k)} \mathbb{E} [\xi_{HP} (P_{\text{in}} - C^O Y(s)) + \xi_P \mid Y(t_k) = y] ds \\ &= \int_{t_k}^{t_{k+1}} (\xi_{HP} P_{\text{in}} + \xi_P) e^{-\delta(s-t_k)} ds - \xi_{HP} C^O \left\{ \int_{t_k}^{t_{k+1}} e^{-\delta(s-t_k)} \left(e^{A(s-t_k)} Y(t_k) + (e^{A(s-t_k)} - \mathbb{I}_\ell) A^{-1} B g(t_k, +1) \right) ds \right\} \\ &= \frac{(\xi_{HP} P_{\text{in}} + \xi_P)}{\delta} (1 - e^{-\delta \Delta_N}) - \xi_{HP} C^O \left\{ (e^{(A - \delta \mathbb{I}_\ell) \Delta_N} - \mathbb{I}_\ell) (A - \delta \mathbb{I}_\ell)^{-1} y \right. \\ &\quad \left. + \left[(e^{(A - \delta \mathbb{I}_\ell) \Delta_N} - \mathbb{I}_\ell) (A - \delta \mathbb{I}_\ell)^{-1} - \frac{1}{\delta} (1 - e^{-\delta \Delta_N}) \mathbb{I}_\ell \right] A^{-1} B g(t_n, +1) \right\}. \end{aligned}$$

Finally, for $a = -1$, we obtain

$$\bar{\Psi}(k, x, a) = \int_{t_k}^{t_{k+1}} e^{-\delta(s-t_k)} \mathbb{E}_{k,x} [\psi(X^{\bar{u}}(s), a)] ds = \xi_P \int_{t_k}^{t_{k+1}} e^{-\delta(s-t_k)} ds = \frac{\xi_P}{\delta} (1 - e^{-\delta \Delta_N}).$$

For $a = 0, -2$ the claim follows from $\psi(x, a) = 0$. □